

DESIGN, FABRICATION AND CHARACTERIZATION OF MEMS  
BASED MICRO HEATER FOR VAPORIZING LIQUID  
MICROTHRUSTER

A thesis submitted to the Delft University of Technology in partial fulfillment  
of the requirements for the degree of

Master of Science in Electrical Engineering

by

Alisher Kurmanbay

June 2019

Alisher Kurmanbay: *Design, Fabrication and Characterization of MEMS based micro heater for Vaporizing Liquid Microthruster* (2019)



The work in this thesis was made in the:



ECTM  
Microelectronics  
Faculty of Microelectronics  
Delft University of Technology

Supervisors:	Prof.dr. G.Q. Zhang Prof.dr. Lina Sarro
Daily Supervisor	Dr. Henk van Zeijl Dr. A.Mirzagheytaghi
Co-reader:	Prof.Dr. B. Zandbergen

## ABSTRACT

Demand and development in the space industry are conditioning more cost-effective satellites without a reduction in functionality. One of the means of satisfying thus requirements is miniaturization. Constructing, smarter, lighter and cheaper satellites to reduce the cost of delivering it to the orbit as the main chunk of mission cost falls on delivering the satellite to space. Lighter versions of satellites called nano-satellites (CubeSats) which could be fabricated in mass scale in a reproducible manner might be a suitable solution. In simple words nanosatellite is a state of the art device packed with advanced logic electronics, sensor and actuator arrays as well as power management systems, etc. to perform numerous tasks. Considering the already high cost for large scale integration of various components it is very important to extend the lifetime of the devices as much as possible. Beside radiation which is one of the main reason for the failure of the components, satellites are useful only if they remain in the orbit and not deviate from the specific path it was set due to drag. Therefore the propulsion system is required to control the altitude to increase the operational lifetime of the satellite.

The project is a continuation of the work in realizing a new generation of noble green Vaporizing Liquid Micro Thruster (VLM) functioning in environmentally friendly propellant(water) fabricated in Else Kooi Laboratory (EKL) with the cooperation of Aerospace Engineering (AE) faculty with an intention of contributing to the DELFFI mission. Thesis includes fabrication and testing of a thruster with a heavy emphasis on improving the performance of the heating chamber. Fabrication was accomplished by designing modules separately and assembling them through part by part exposure in the lithography. Such an approach was taken due to the need for systematic analysis of numerous factors affecting performance by altering them and observe the effect on performance. Several heating chambers were designed with varying performance attributes and tested on its ability to deliver heat efficiently as well as affect to thruster performance like pressure drop. In addition to it, several fabrication techniques not used previously for the fabrication of thrusters were experimented and implemented on making various channel structures giving freedom of more 3D design.

As a result novel type of Microelectromechanical Systems (MEMS) VLM heating chambers were fabricated by modular design and tested. Developed process is robust and flexible which allows to manufacture different types of VLM thrusters depending on operation demand and suited for integration. The novelty introduced in the project is step-wise heating as well as the application of a new type of localized heating chamber with improved geometry for enhanced heating efficiency and for wall temperature measurements.





## ACKNOWLEDGEMENTS

I would like to thank my super duper visor Henk van Zeijl for introducing me to the world of MEMS and making this project possible. I will always appreciate your patience and wise guidance as well as protection in all stages of the project. I was continuously fascinated by your methodology of explaining complex things in a maximum compact and affordable to students way. You are a great teacher.

I will never forget help received from extremely intelligent PhDs and post-docs. Bruno, Amir, Ibrahim, Juan. Thanks a lot with a theory and lab help. I appreciate a lot that you guys are here in ECTM and kind enough to guide us. I cordially wish you a big success in the future works.

I would also like to show my deepest appreciation and cordial thanks to EKL personal who were very supportive and altruistically helping in speeding up the process and sharing knowledge about the challenging world of MEMS. The project would be impossible without techniques and recipes developed by skillful engineers over many years and I am very grateful that thus accumulated knowledge was shared to give me incredible opportunities and extremely brave design choices.

Over the span of a master, I had a chance to be an office-mate of wonderful people. I would like to thank them for their warm talks and help in the areas I didn't master. Raj, Mike, Hu, Dong thanks a lot for your help. I would never forget that.

I met a lot of amazing people outside of my department as well. Fellow Ms students going through the same path. Andrei, Arthur, Marios, Antonio, Vlad, Pat, Nikita, Hassan, Yusuf, Sergei, Mateusz, Ahmed. Thanks a lot for the warm and interesting discussions we had.

During the Ms period, I received a lot of support from my best friends with whom I grew up since middle school. My bros Miras, Anuar love you guys!

Support of my family was one of the most important factors in the realization of this project and my personal existence. I thank my family and their prayers and sincere love which was the most influential factor for me to make sense of daily life.

Above all, I give my thanks to Almighty God, from whom all the blessings are. Faith is the core of my thinking and light of guidance as a passenger in this world. May my all future work to be dedicated to fulfilling my mission according to his will, and be a testament to his infinite glory.

...



# CONTENTS

1	INTRODUCTION	1
1.1	Project Background	1
1.1.1	VLM as a concept	4
1.1.2	Modules of the VLM	5
1.1.3	Performance of the VLM	6
1.2	Literature Review on Previous Designs	9
1.2.1	Internal Micro Channel (heater)	10
1.2.2	External Heat Source	12
1.2.3	Lessons Learned	13
1.3	Chapter Summary	14
2	DESIGN APPROACH	15
2.1	Concept and Theory	15
2.1.1	External DC heat source	15
2.1.2	Internal Channel Structure	17
2.1.3	Power Consumption Estimates	20
2.2	Design Restrictions (Requirements)	22
2.3	Design Proposal (VLM Architecture)	23
2.3.1	Uniformity	26
2.3.2	Flow Instability Mitigation attempt	26
2.4	Chapter Summary	28
3	MODEL VERIFICATION	29
3.1	Geometry and Meshing	29
3.2	Boundary Conditions	29
3.3	Data Generated	31
3.4	Electra Thermal Model	32
3.5	Chapter Summary	34
4	FABRICATION	37
4.1	Modular Fabrication	38
4.2	Processing	39
4.2.1	Front side processing	39
4.2.2	Back side Processing	40
4.2.3	Expansion on DRIE	41
4.2.4	Anodic Bonding	43
4.2.5	Connection to microfluidic interface	44
4.2.6	Challenges during Fabrication	45
4.3	Chapter Summary	47
5	CHARACTERIZATION	49
5.1	Experimental Setup	49
5.2	Electra - Thermal Characterization	51
5.2.1	Process control - Sheet Resistance	51
5.2.2	Wafer level measurements for Resistive Temperature Detector (RTD) calibration	52
5.2.3	Thermal Resistance	53
5.2.4	Time constant	55
5.3	Pressure drop across various channel structures	56

5.4	Visual Observation . . . . .	57
5.4.1	Observation of flow regimes . . . . .	57
5.4.2	Possible Criterion for the flow stability . . . . .	58
5.4.3	Discussion on wall temperature uniformity . . . . .	59
5.5	Chapter Summary . . . . .	60
6	SUMMARY . . . . .	61
6.1	Conclusion . . . . .	61
6.2	Further Research . . . . .	64
6.3	Possible applications other than VLM . . . . .	67
A	APPENDIX A (DELFFI REQUIREMENTS) . . . . .	73
B	APPENDIX B (FLOW CHART) . . . . .	75
C	APPENDIX C (HEATERS & CHANNELS ) . . . . .	79
D	APPENDIX D (MASK ) . . . . .	83
E	ETHICS . . . . .	87
F	* . . . . .	89

## LIST OF FIGURES

Figure 1.1	Schematic of VLM thruster with numerated modules [28] . . . . .	4
Figure 1.2	Various channel structures experimented in the past . . . . .	9
Figure 1.3	Example of diamond shaped internal channel geometry [8] . . . . .	10
Figure 1.4	Major Causes of multi phase flow bubbling instabilities [36] . . . . .	11
Figure 1.5	Example of micro heater for gas sensing [21] with high temperature compatibility . . . . .	12
Figure 2.1	Average Nusselt's Number under constant wall temperature and product of friction factor & Re based on hydraulic diameter [30] . . . . .	18
Figure 2.2	Heat transfer and pressure drop across staggered row structures (Re = 500) as described by [11] . . . . .	20
Figure 2.3	Heat transfer and pressure drop across periodic channel (Re = 474.6) as described by [19] . . . . .	21
Figure 2.4	Minimal Power to Reach vaporization for a given flow rate [mg/s] . . . . .	22
Figure 2.5	Design side view and cross sections . . . . .	24
Figure 2.6	Thermal resistance network . . . . .	24
Figure 2.7	Rise of thermal resistance by etching hexagonal pattern. . . . .	26
Figure 2.8	Illustration of uniformity achieved . . . . .	27
Figure 2.9	Design representation . . . . .	27
Figure 3.1	Digital model of the device . . . . .	30
Figure 3.2	Cumulative flux of energy through all faces of the single element has to equal to zero . . . . .	31
Figure 3.3	Power inputed to heat source and equivalent wall temperature of high aspect ratio fins. . . . .	33
Figure 3.4	Power inputed to heat source and equivalent wall temperature of conventional fins. . . . .	33
Figure 3.5	Normalized thermal resistance comparison . . . . .	34
Figure 4.1	Visualization of the possible combinations which could be extracted by using modular design . . . . .	38
Figure 4.2	Several Example of what could be extracted using modular design while total combination could be extracted is virtually infinite . . . . .	39
Figure 4.3	Process steps for front side fabrication . . . . .	40
Figure 4.4	Process steps for back side fabrication . . . . .	41
Figure 4.5	Heater parts . . . . .	42
Figure 4.6	Keyence 3D microscope capture of the fin structure (backside of the wafer). Multiple step deepness could be observed where the deepest parts going all the way to $250\mu m$ . . . . .	42
Figure 4.7	Front side Deep Reactive Ion Etching (DRIE) processing procedure visualized . . . . .	43
Figure 4.8	Scanning Electron Microscope (SEM) capture of the chamber cross section and nozzle for quality evaluation . . . . .	44

Figure 4.9	Side view of individual die connected to the microfluidic interface and attached to the PCB with the 3D printing support for more reliable handling . . . . .	44
Figure 4.10	Heater parts . . . . .	45
Figure 4.11	Keyence 3D microscope capture of roughness created after DRIE due to fall off of photoresist. This however was observed in several devices didn't spread to whole wafer. Reason for poor adhesiveness of the AZ-12-XT20PL photoresist could be the patterned Plasma Enhanced Chemical Vapour Deposition (PECVD) Tetraethyl orthosilicate (TEOS) layer(hard mask). Topography of which prevented good adhesiveness. . .	46
Figure 4.12	Oxidation happened after the heater was heated up to high temperature ( $600C^0$ ) this resulted in formation of hot spots as resistance at the high concentration of pinholes grew significantly . . . . .	46
Figure 4.13	Front side picture of finished product, presented with a penny in the background (diameter of which is $19.05mm$ ). . . . .	47
Figure 5.1	Experimental setup for the heater characterization . .	49
Figure 5.2	Pin assignment, dimensions and routing of the custom Portable Circuit Board (PCB) designed for the VLM measurements. Design of the VLM includes Pyrex wafer as a bottom insulation and it is expected that it will serve as good insulation layer, removing any need for additional heat protecting measures in PCB design. Pins for VLM connections are made of Au as its suitable metal for wire bonding. . . . .	50
Figure 5.3	Van der Pauw structure . . . . .	51
Figure 5.4	Calibration curve of all heaters (images of each heater could be viewed from Appendix A) . . . . .	52
Figure 5.5	Temperature Response of the $CH_4$ (dry) for the given power input . . . . .	53
Figure 5.6	Temperature Response of the $CH_2$ (dry) for the given power input . . . . .	53
Figure 5.7	Temperature Response of the $CH_4$ (wet [ $0.25\text{ g/s}$ ]) for the given power input . . . . .	54
Figure 5.8	Temperature Response of the $CH_2$ (wet [ $0.25\text{ g/s}$ ]) for the given power input . . . . .	54
Figure 5.9	Heating efficiency as well as removed heat flux to the propellant at the flow of $0.25\text{g/s}$ . . . . .	55
Figure 5.10	EPCOS2013 [10] mounted on top of the VLM . . . . .	56
Figure 5.11	Visual inspection of flow at high power of $5[W]$ . . .	57
Figure 5.12	Visual inspection of bubble formation for the flow rate of $0.25[\text{g/s}]$ and power supply of $2[W]$ . . . . .	58
Figure 5.13	Preheated middle heater at $343C^0$ is a gate through which the water is converted into vapour form. . . .	59
Figure 5.14	When $6.5[W]$ was applied to preheat 1st heater (right most) to achieve $454C^0$ the last fin structures (left most wall) showed $215C^0$ . . . . .	59
Figure 6.1	(a) - (b) Channel geometry with internally hollow structure (c) Channel geometry with varying structures . . . . .	64

Figure 6.2	Packaged device concept . . . . .	65
Figure 6.3	Packaged device with temperature sensor . . . . .	66
Figure C.1	Heater 1 . . . . .	79
Figure C.2	Heater 2 . . . . .	79
Figure C.3	Heater 3 . . . . .	79
Figure C.4	Heater 4 . . . . .	80
Figure C.5	Channel 1 Microscope capture . . . . .	80
Figure C.6	Channel 2 Microscope capture . . . . .	81
Figure C.7	Channel 3 Microscope capture . . . . .	81
Figure C.8	Channel 4 Microscope capture . . . . .	81
Figure C.9	Channel 5 Microscope capture . . . . .	81
Figure C.10	Channel 6 Microscope capture . . . . .	82
Figure C.11	Channel 7 Microscope capture . . . . .	82
Figure D.1	Mask Top Cell . . . . .	83
Figure D.2	Wafer level organization of the devices. Each square inch of the wafer was attempted to be used to get max amount of devices. Wafer is organized in a symmetric way around y axis to avoid lithography errors in alignment. Proposed combinations are not limit and if desired much bigger thrusters could be assembled.	84





## LIST OF TABLES

Table 1.1	Weighting of workload for realization of VLM . . . . .	2
Table 1.2	Some possible alternatives to the propellant. [25] For the safety in the lab only water is tested. . . . .	8
Table 2.1	Table with major attributes of temperature detecting methods [9]. RTD was chosen due to large temperature range and quick thermal response compared to other measuring methods. . . . .	16
Table 2.2	Several important material parameters suitable of serving as a heater/RTD . . . . .	17
Table 3.1	Boundary conditions for elements based on heat transfer equations 3.1 - 3.4 (0 is denoted for insulation bottom glass). Corner elements are computed in similar fashion. Given large number of elements the error introduced by corner elements are negligible. Nevertheless, they are taken into account. for meshing used for this particular simulation computation are performed based on normal direction to the surface. . . . .	32
Table 5.1	Table representing values of sheet resistance measured directly after metalization step . . . . .	51
Table 5.2	Heat removal across the channels at 2W . . . . .	55
Table C.1	Table with nomenclature and description of a heaters here H is length of one meander . . . . .	80
Table C.2	Table with nomenclature and description of a channels . . . . .	82



## ACRONYMS

<b>MEMS</b>	Microelectromechanical Systems	iii
<b>VLM</b>	Vaporizing Liquid Micro Thruster	iii
<b>EKL</b>	Else Kooi Laboratory	iii
<b>ECTM</b>	Electronic Components, Technology and Materials	2
<b>TCR</b>	Temperature Coefficient of Resistance	16
<b>DRIE</b>	Deep Reactive Ion Etching	ix
<b>AE</b>	Aerospace Engineering	iii
<b>3ME</b>	Mechanical, Maritime and Materials Engineering	5
<b>RTD</b>	Resistive Temperature Detector	vii
<b>MP</b>	Melting Point	15
<b>LPCVD</b>	Low Pressure Chemical Vapour Deposition	37
<b>PECVD</b>	Plasma Enhanced Chemical Vapour Deposition	x
<b>PR</b>	Photo Resist	40
<b>RIE</b>	Reactive Ion Etching	37
<b>TEOS</b>	Tetraethyl orthosilicate	x
<b>PCB</b>	Portable Circuit Board	x
<b>SEM</b>	Scanning Electron Microscope	ix



# 1 | INTRODUCTION

*"...Out of darkness into light"*

---

## 1.1 PROJECT BACKGROUND

Since the first transistor was characterized by Bardeen, Brattain, and Shockley in Bell's lab, semiconductor industry saw immense growth and from the very beginning, it was moving towards manufacturing faster, miniaturized and cost-effective dense structures. Today it is hard to imagine a field which hasn't been affected by it. Although Moore's law started to lose its accuracy and it seems like miniaturization reached its limits, fabricating smaller, smarter and cheaper devices for a various application other than transistors is a field which didn't reach its maturity yet. In this essence knowledge accumulated in the semiconductor industry plays a critical role in bringing smarter MEMS into life. As times go by MEMS conquer more and more scientific and industrial spheres. It even found application in manufacturing of micro-propulsion systems where a fluid is accelerated to supersonic speed in microscale. A new type of satellites called CubeSats or nanosatellites which can be produced in a reproducible manner needs thus propulsion systems for altitude control. TU Delft is working towards accomplishing DELFFI mission: an experimental flight of 'Delta' and 'Phi' nanosatellites made in Delft to the orbit of LEO. System analysis of nanosatellites will show high complexity of the satellite, consisting of numerous systems, each of which is the system itself. Such a very large scale integration of systems will allow replacing some of the functions of bulky, extremely expensive and hardly-reproducible satellites produced today, opening doors for affordable space exploration. However, due to still strong air drag in the LEO which is hard to model [27] nano-satellites needs controllable and reliable propulsion system. VLM is one of the main candidates for taking its place as miniature reliable as well as an environmentally safe mini engine. Topics touched in the thesis could be used not only for propulsion system but also be useful for another challenge that raises concern in the design of the CubeSats. Highly integrated densely populated electronics needs adequate thermal management, which can not be accomplished by traditional natural or forced convective cooling methods due to the absence of the air in the space. Multiphase phenomena are very actively researched topic in recent years, and every new design whether for a specific application or for fundamental studies has the potential to be an interesting solution for existing problems of the thermal domain. Therefore, principles and fabrication techniques used in the design of the heating chamber could be used for temperature management of the electronic circuits as well.

*Thesis Objective*

The main objective of the thesis is to discuss MEMS techniques used to miniaturize VLM as well as attempts towards enhancing its performance. Specifically, the focus is towards the design and fabrication of the micro heating chamber which was accomplished in the EKL clean room. During the span of the project, heat transfer modes were studied and based on the best predictions several designs of the heating chamber were made and tested on the parameters like efficiency, practicality, and effect on the performance of the VLM. Fabrication techniques previously not used in VLM production were tested and implemented to enhance the performance attributes to contribute overall performance and consequently satisfy mission requirements. Fabrication process developed represents a wide spectrum of various MEMS techniques and leave some space for further improvements if necessary.

Workload	Points [out of 10]
1. Concept & System analysis	2
2. Design & Realization efforts	2
<b>3. Fabrication efforts</b>	<b>4</b>
4. Characterization & Verification	2

**Table 1.1:** Weighting of workload for realization of VLM

The organization of workload is a crucial part of any project dedicated to realizing a product. However, division of importance for sections of the VLM workload was done on the level of proficiency researcher have on each category and based on the boundaries of the project timeline as well as taking into considerations financial resources it would require. As a student of Electronic Components, Technology and Materials (ECTM), the most focus was done on fabrication as it could be seen from the point distribution. However, fabrication efforts spent in this research believed to possess potential to improve the design, make characterization of the future devices easier and allow exploring possible performance enhancement. The heating chamber was adapted to be suitable for integration with other modules of the VLM and therefore high priority was given to flexibility and robustness of the fabrication. The weighting of the efforts that will be spent on the realization of the heating chamber is shown as a short summary in table 1.1.

### *Thesis Questions*

To clarify the research objective more in-depth, the most important research questions are presented. It has to be noted that in the realization of VLM concept there were thesis objectives which contradicted each other and necessity of design with a trade off depending on importance had to be made. In this project foremost important factors are the enhancement of heating efficiency and reducing pressure drop through the chamber, therefore in case of conflict in the objective, the decision was done in favor of thus two. However, the realization of both requirement is not possible as well as it will be seen later, enhancement of one is often followed by reduction of the other.

1. Investigate the VLM as a system and describe the performance attributes in a mathematical model. (based on the literature and past projects done in TU Delft).
2. Investigate methods of system orthogonalization into independent parts for straightforward analysis and modular design efforts.
3. Investigate possible means of improving heating efficiency. (the foremost important task of the research).
4. Investigate deriving proper heat sink shape or other means of making VLM heating chamber isothermal and stable.
5. Investigate options of achieving a non-intrusive design of chamber for reduction of pressure (thrust) losses.
6. Investigate solutions of achieving more compact (miniaturized) VLM and subsequent reduction of mass and volume without a reduction in functionality.
7. Investigate feasibility of fabrication to achieve the above tasks.
8. Investigate mathematical solutions to describe the behavior of the designed device.
9. Investigate back end options(packaging) of the final product without affecting performance in a negative way.
10. Investigate options for conducting non-intrusive experiment techniques to verify functionality.

## 1.1.1 VLM as a concept

When it comes to micro-propulsion systems for nanosatellites, variety of thrust options functioning on solid [17],[35],etc. vaporising liquid [22],[3],etc., gas [16] as well as on ion [4] source exists. One of the promising options that could take its place on that race is VLM, which not only has good performance but also can operate on safe, cheap and environmentally friendly propellants. Advantages of the VLM are its relatively simple fabrication which could be done using conventional MEMS techniques as well as the absence of moving parts which increases its reliability and consequently operational lifetime. Furthermore, using MEMS techniques VLM could be downsized to the extreme limit, allowing incredibly lightweight miniature propulsion solution, which is among the main advantage comparing to the competing solutions.

However, VLM has its weaknesses as well. In terms of energy, it is quite difficult to vaporize water due to its latent heat of vaporization. In addition to it, the necessity of external power source for powering VLM as well as the presence of liquid propellant adds up to the overall weight of the satellite. In this project, VLM is partitioned into several modules for ease of analysis and for a more in-depth overview of the effect of the individual VLM section on the performance. Each module would be attempted to be developed and optimized separately and integrated later on. Such a measure is taken out of extreme complexity of the physical phenomenons taking place inside the VLM requiring huge resources and manpower for the realization.



Figure 1.1: Schematic of VLM thruster with numerated modules [28]

- |                            |                           |
|----------------------------|---------------------------|
| 1. Propellant inlet        | 4. Nozzle convergent area |
| 2. Divergent inlet section | 5. Nozzle throat          |
| 3. <b>Heating Chamber</b>  | 6. Nozzle diverging area  |

Although improving performance in microscale doesn't always improve overall performance, if modules are orthogonalized correctly (independent factors of each module is derived precisely and known) performance boost in macro-scale could be expected. As it was mentioned before in this work efforts would be spent on researching the heating chamber and the other modules are analyzed to extract input-output parameters of the VLM heating chamber.



### 1.1.2 Modules of the VLM

#### *Inlet*

Purpose of this module is to deliver propellant to VLM in an efficient and controlled manner without too much reduction in pressure. Importance of this part is that how the heat will be accepted by the propellant in the heating chamber will depend on how the flow is introduced. One of the functionalities of an inlet section is a smooth interconnect between microfluidic interface and the VLM itself. Any potential leakage is unacceptable and will cancel the functionality of the remaining modules. Studies on improving this module are going on in Mechanical, Maritime and Materials Engineering (3ME) faculty. Inlet section might include complex solutions, for instance, implementation of TESLA valves were accomplished in [26] which were designed to suppress backflow.

#### *Heating Chamber*

In this module, the propellant is heated up and converted into vapor form. Expansion of the propellant due to change of density creates pressure increase which propels the water towards nozzle along with inlet (input) pressure. While in the vapor form viscous losses are reduced. Rise of temperature is important for  $I_{sp}$  as it could be seen from equation 1.4 that velocity has temperature dependency. Heating chamber itself could be separated into two distinct parts channel section through which propellant absorbs energy and external DC heat source which generates Joule Heat. Each, part of the heating chamber, is equally important and design choices would be discussed in Chapter 2 Main requirement for this module is an ability to deliver the Joule heat generated by source to the propellant and create as less pressure drop as possible. Thermally insulating package of the whole thruster could be included in this part as well, as it directly affects the performance of the heating chamber.

#### *Nozzle*

Vaporized water is accelerated towards the throat and pushed out of the VLM creating thrust. The geometry of the Nozzle plays a crucial role in dictating the way propellant exits the chamber. Design of the nozzle should be done in a way that liquid exiting the throat of the nozzle should gain maximum allowed speed (impulse) to generate high thrust. Depending on propellant and thrust requirements linear or air-spike nozzles could be integrated into the VLM. This module is being developed in AE and numerical and experimental studies are actively pushed forward. Nozzle fabrication requirements might be quite different and development of the heating chamber and inlet should consider it carefully. In this project standard linear nozzle was integrated to the chamber to test the possibility to fabricate them together. However, the effect of nozzle to performance was not a point of concern and variables affecting the performance were not tested.

## 1.1.3 Performance of the VLM

*Overall Performance*

When describing the performance of the thruster the key property by which thruster is valued is the amount of thrust it can output. In other words, thrust is the force VLM is pulling the satellite which is generated by conversion of electrical energy into mechanical. In modular design, it is important to orthogonalize the performance aspects of each module correctly in order to preserve overall performance quality. Ideal thrust is described as in equation 1.1

$$F = \dot{m}v_e + (p_e - p_a)A_e \quad (1.1)$$

Where:

$\dot{m}$  - is mass flow rate

$v_e$  - is exit velocity

$p_e$  - exit pressure

$p_a$  - ambient pressure

$A_e$  - nozzle exit area

From the above expression, two components affecting thrust could be extracted. Mass flow rate, velocity (momentum) and chamber ambient pressure difference. In designing heating chamber module priority should be not affecting these parameters in a negative way. To confirm this statement it is worth to look at paraphrased ideal thrust equation which is a function of the pressure only [3] where temperature cancels out momentum as seen from the equation 1.2:

$$F = v_e^2 A_e + p_e A_e \quad (1.2)$$

Moving further another important performance parameter is specific impulse - the amount of force generated per unit weight of the propellant used. It could be understood as thrust efficiency and described as in equation 1.3:

$$I_{sp} = \frac{F}{\dot{m}g} = \frac{v_e}{g} \quad (1.3)$$

Here  $g$  is gravitational constant.

It is time to look at governing equations of the exit velocity as it could be seen that thrust is directly dependent on this important parameter. Equation 1.4 describes exit velocity of the vaporized liquid.

$$v_e = \sqrt{\frac{2\gamma}{\gamma-1}RT_c(1 - (\frac{p_e}{p_c})^{\frac{\gamma-1}{\gamma}})} \quad (1.4)$$

Here:

$\gamma$  - specific heat ratio of the propellant

$R$  - gas constant of the propellant

$T_c$  - is chamber temperature

$p_c$  - is chamber pressure

Although, fluid chosen for this project is fixed water - an environmentally friendly substance which doesn't pose a chemical danger. It could be noticed from the above equations propellant has a profound impact on the

performance where viscous losses are governed by the propellant and at a throat Reynolds number could be written by the equation 1.5:

$$Re = v_t D_t \frac{\rho_t}{\mu_t} = \frac{\dot{m}}{\mu h_0} \quad (1.5)$$

Here:

$D_t$  - throat width

$h_0$  - throat height

$\mu_t$  - viscosity at throat

$\rho_t$  - density at throat

Another propellant properties governing operation of the VLM are described by fundamental fluid equations 1.6 - 1.7:

$$Nu = h \frac{D}{k_f} \quad (1.6)$$

$$Pr = \mu \frac{C_p}{k_f} \quad (1.7)$$

Where:

$D$  - hydrolic diameter

$h$  - heat transfer coefficient

$C_p$  - cpecific heat capacity

$k_f$  - thermal conductivity

One more way of describing how propellant affects the thrust could be seen when thrust is expressed as in equation 1.8:

$$F \propto \dot{m} v_e \propto Re h_0 \mu_t v_e \quad (1.8)$$

Water is not the perfect liquid to serve as the propellant in terms of energy concerns as it has very high latent heat of vaporization which requires extreme energy to overcome. In terms of numbers, it requires eight times more energy for the phase transition to occur than reaching a critical point of vaporization. Only after that benefit of reduction of viscous losses can be experienced. However, the propulsion system could be integrated with the high power electronics in the satellite to remove heat and thus can be used as preheating to save energy.

Although, many cold gas thrusters claim to posses a potential to be VLM once operated with water, as it was found out during the project, it is not completely possible. The VLM architecture has to be completely different as mulit-phase flow has its unique challenges and accompanied with boiling instability phenomenon. Nevertheless, for the successful VLM architecture other liquids with smaller latent heat of vaporization (energy efficiency) and small molecular weight (bigger  $I_{sp}$ ) could be applied. For instance ammonia could be a good candidate for that. Chamber dimensions still has to be modified and optimized for the new liquid.

Propellant	Formula	Liquid density	Latent Heat
Ammonia	$NH_3$	$0.6 \text{ g/cm}^3$	$1159.7 \text{ kJ/kg}$
Propane	$C_3H_8$	$0.49 \text{ g/cm}^3$	$339.3 \text{ kJ/kg}$
Ethyl Chloride	$C_2H_5Cl$	$0.92 \text{ g/cm}^3$	$388.1 \text{ kJ/kg}$
Butane	$C_4H_{10}$	$0.57 \text{ g/cm}^3$	$360.2 \text{ kJ/kg}$
Freon 12	$CCl_2F_2$	$0.98 \text{ g/cm}^3$	$141.8 \text{ kJ/kg}$
<b>Water</b>	$H_2O$	<b><math>1.00 \text{ g/cm}^3</math></b>	<b><math>2442.5 \text{ kJ/kg}</math></b>
Hydrogen Fluoride	$HF$	$0.99 \text{ g/cm}^3$	$1505.9 \text{ kJ/kg}$
Methanol	$C_2H_5OH$	$0.79 \text{ g/cm}^3$	$1099.3 \text{ kJ/kg}$
Methyl Chloride	$CH_3OH$	$0.91 \text{ g/cm}^3$	$376.5 \text{ kJ/kg}$
Ethane	$C_2H_6$	$0.56 \text{ g/cm}^3$	$313.7 \text{ kJ/kg}$
Ethyl Methyl Ether	$C_2H_5OCH_3$	$0.80 \text{ g/cm}^3$	$350.9 \text{ kJ/kg}$
Mono Methyl Amine	$CH_3NH_2$	$0.77 \text{ g/cm}^3$	$873.8 \text{ kJ/kg}$

**Table 1.2:** Some possible alternatives to the propellant. [25] For the safety in the lab only water is tested.

### Heater Performance

In characterizing the heater performance knowing precise heat distribution is essential. Involvement of flow makes analytic solutions very difficult if not impossible. In addition to it, uncertainty in geometry in micro-scale due to process, variations might influence the solution making it invaluable. Therefore, empirical results and/or numerical simulations of the full thruster is required. Overall, heater performance would be evaluated by power consumption efficiency as expressed in equation 1.9:

$$\eta = \frac{P_{propellant}}{P_{electrical}} \quad (1.9)$$

where:

$$P_{propellant} = P_{liquid\Delta T} + P_{evap} + P_{gas\Delta T} \quad (1.10)$$

$P_{propellant}$  - power delivered to the propellant

$P_{liquid\Delta T}$  - power spent on rising temperature of the liquid

$P_{gas\Delta T}$  - power spent on rising the temperature of the propellant above vaporization point

$P_{evap}$  - power spent on overcoming latent phase

While thermal efficiency is commonly expressed as in equation 1.11

$$\epsilon = \frac{T_{fluid,exit} - T_{fluid,inlet}}{T_{wall,exit} - T_{fluid,inlet}} \quad (1.11)$$

It has to be noted that temperature inside the chamber is highly nonuniform and for performance characterization, the only equivalent temperature has importance.

## 1.2 LITERATURE REVIEW ON PREVIOUS DESIGNS

Design of the VLM is ever improving process and evolution of the VLM design were carefully studied and lessons learned from previous designs were taken into account to improve the design as much as possible. One of the main challenges reported by many researchers [3],[34],[12],[23] were heater stability issue. The effect was described as *sputtering*: the nature of the cause is not well known but it was observed that most likely due to non-uniform heat distribution from the source, hot-spots were formed which created local pressure drop and prevented free movement of the propellant. Moreover, this effect could be observed visually as hot spots were a reason for early bubble formation which later on exploded pushing the propellant towards inlet rather than towards nozzle. In presenting the previous designs unavoidable partitioning is used. Designs would be presented classified into two sections:

1. Internal Heater. (Fin Structure)
2. External Heat source (Resistive Heater)

\*Internal heat sources are also possible, such brave options were experimented by [34]. Challenges that arose were the reliability of such devices as internal heaters have to be connected to outside electronics which not only makes bonding hermetic but, also limits material choice which shouldn't go into chemical reaction with water. In addition to its physical sturdiness of the heater is put under test as propellant accelerated towards nozzle introduce physical stress on it. Moreover, the performance improvement was not noticed due to the small heater surface of contact with a propellant.

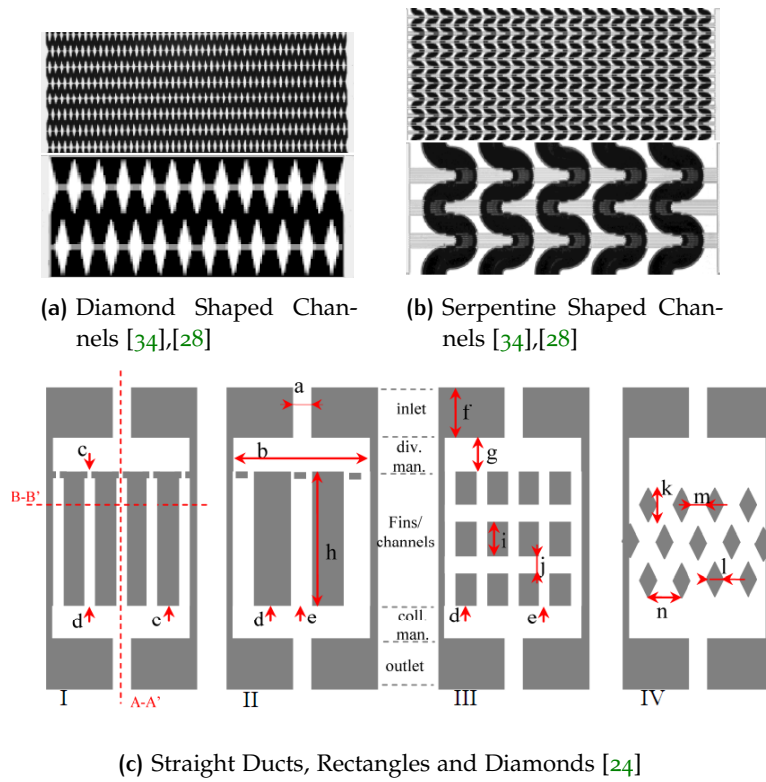
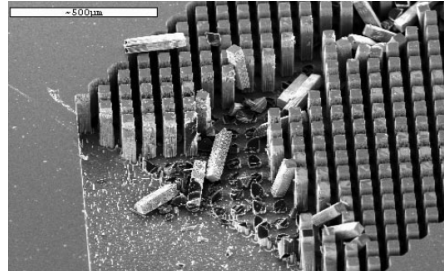


Figure 1.2: Various channel structures experimented in the past



**Figure 1.3:** Example of diamond shaped internal channel geometry [8]

#### 1.2.1 Internal Micro Channel (heater)

In an attempt to find promising heater geometry to deliver heat in the most efficient manner possible various heater geometries have been experimented in the past. However, their characterization was done in a limited manner due to the difficulty of mathematical characterization and involvement of multiphysics phenomenons. In 1981 with the assumption of laminar flow heat transfer parameters in the straight ducts at a single phase flow was characterized by [33]. Numerical and experimental characterization of straight channels with application in the propulsion system was done by [3]. Later, it was shown numerically and experimentally by [11], [19] that periodic structures in the channel were propellant sees expansion and contraction proven to improve heat transfer characteristics of the channel by a considerable amount (around 20%). In Figure 1.2, several examples of fin structures from past works are shown. This part of the VLM is the major theoretical challenge of the project as analytical solutions to come up with efficient fin structure is not possible, furthermore computational resources for the structure where phase transition occurs are very demanding.

### *Internal Channel structure related failure Modes*

**Bubbling related failure modes** - Multiphase is a complex phenomenon which is not completely understood up to this day. However, a summary of visual observation of failure mechanisms suggests that multiple failure modes could be faced in case of improper design. It might be possible that for each channel there is only a specific operation range with tolerable stability. Several examples of flow instabilities could be shown in the 1.4. Channel geometry is the most researched method of reduction of flow instability. However, significant and consistent attempts on these directions should be made to achieve smooth and stable operation in the microchannels. Unfortunately, the current heat transfer theory cannot offer direct guidelines on the design of the microchannels and most of the VLM available in the literature do not even mention the failure modes.

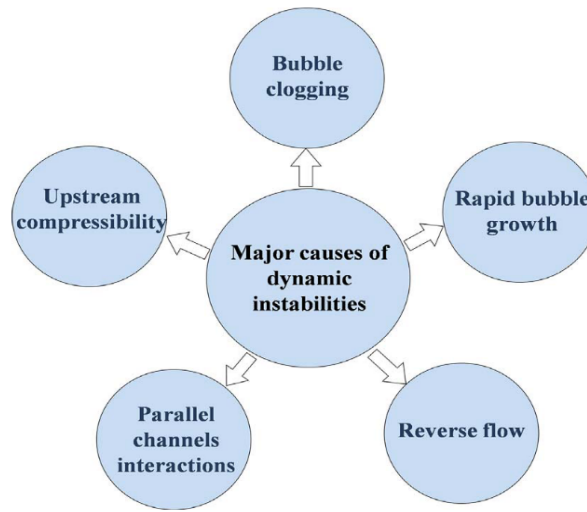
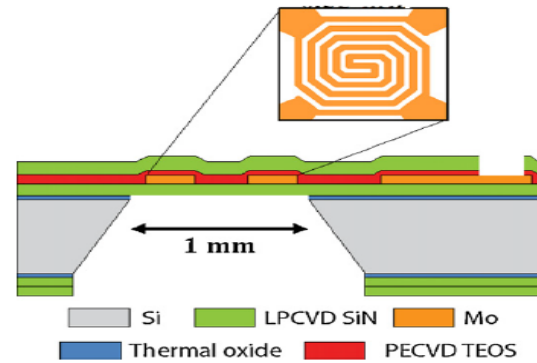


Figure 1.4: Major Causes of multi phase flow bubbling instabilities [36]

**Pressure instabilities related failure modes** - among the flow instability studies, it was observed that it is quite prevalent that pressure oscillations might be undesirable for flow stability [36]. Local pressure drop might influence the outcome of flow stability very much as it will be equivalent of physical obstacle on the path of the flow. Therefore as an attempt to study thus pressure oscillations, it might be useful to investigate options of implementing the pressure sensors or come up with means of measuring the pressure variation across the channel. Once more the channel geometry is the key factor dictating the physical phenomena taking place inside the microchannels. Therefore for each geometry pressure instabilities needs to be recorded and observed with deep care to avoid the VLMS thrust inconsistency.

### 1.2.2 External Heat Source

External heaters have many applications in the sensor industry and commonly used for gas sensing [21],[14],[20]. Fabrication methodology of the hotplates and micro-heaters is a quite mature field. In the EKL large amount of thermal devices were fabricated and when it comes to materials and fabrication enormous experience of ECTM department and EKL was extremely useful (figure 1.5). Examples of extremely low power and accurate heating/sensing micro-hotplates, nanoreactors, etc. with advanced fabrication solutions were available for the analysis. For electrical sensing of the physical phenomena happening inside the chamber, it is very important to have an adequately sensitive and reliable sensing unit. However, when it comes to characterizing power distribution it is quite difficult to find literature which precisely describes heat transfer modes and how to model heater with appropriate geometry and characteristics. Only several information could be found on modeling power distribution [13]. Requirements for the external heater is quite demanding as it is the foremost important section of the heating chamber. Power limitation and accuracy of the temperature measurements, as well as durability and process complexity, are conditioned by the external heater. Therefore, material choice for the heater and at the same time precise temperature detector is a challenging choice. In Chapter 2 external heater would be discussed in more detail and based on the analysis material choice and design considerations would be justified. However, due to the absence of the air in the space, dimensions of the heaters were not the main priority as free vacuum provided in space allows to simplify the heat transfer modes removing the convection to the air completely.



**Figure 1.5:** Example of micro heater for gas sensing [21] with high temperature compatibility

\*Importance of the material choice when it comes to the extremely demanding application cannot be ignored. Operation ranges and abilities of the VLM are often dictated by materials used. A large set of factors like thermal budget, compatibility of elements, their vulnerability to the environment exposed as well as electrical performance has to be studied up to the degree to satisfy the requirements of the VLM.



### 1.2.3 Lessons Learned

#### *Overcoming computational challenges*

An attempt towards delivering the heat in a uniform manner should be made to reduce the risk of *sputtering*. The task, however, is extremely challenging computation-wise and finite element numerical estimation of various geometries needs to be performed to find effective heat transfer parameters and optimal pressure drop. This analysis should reveal temperature and pressure distribution and point on weak spots created by improper design. As a result design of the fin structure which has desired balance between pressure and heating efficiency should be made. This problem has to be solved, however, as for now boundaries distinguishing compact, efficient and non-intrusive design is not set clearly, and up to this moment, there is close to no literature which provides optimal design considerations. Current status of heat transfer theory in microscale cannot offer direct solutions, therefore trial and error of fabricating structures and testing their validity is the only possibility. Two-phase flow is accompanied with instabilities *sputtering* without resolving of which thruster cannot operate in stable operation mode. The effect of thus instabilities is the point of interest of current leading thermal mass transport studies [32],[36]. It is quite possible that even with the realization of the uniform heat distribution the range of stable operation regime might be very narrow and only at specific supply pressure and at predefined heat transfer rates constant thrust could be expected.

#### *Need of control circuitry for further development of the project*

Advances in manufacturing techniques allowed to shift focus more on performance and effectively monitoring and controlling performance actively. This requires robust circuitry and advanced understanding of the heat transfer and fluid dynamics in microscale. It was observed in many studies [34],[12] for VLM it takes a considerable amount of time to reach steady state operation while maintaining thruster stability is not attempted in most of the researches conducted. Operating in the pulsated mode, for instance, is not possible without advanced active control. Therefore online information about processes taking places inside the chamber is required. However, this is out of the reach goals for Ms project. Nevertheless, characterizing heater performance and obtaining valuable information about the physical process taking place inside the VLM is an attempt towards active control.

#### *Importance of working from the front end and back end*

One of the conclusions of the researches investigated VLM and heaters, in general, is the importance of packaging and making the design suitable for comfortable operation without loss in performance. It is important to work from the front end and back end to realize the functional product. Furthermore, several characteristics of VLM could be verified reliably only once some of the parasitic effects of the performance is nullified by proper packaging. In addition to it, the designed chip shouldn't be too fragile to handle during the characterization, as mechanical stress during connections to the microfluidic and electrical interface is unavoidable. Therefore, packaging of the device should be placed in high priority and considerable design efforts should be spent towards realizing more complete product with packaging as a central part of working towards enhancing functionality.

### 1.3 CHAPTER SUMMARY

In this Chapter 1 project background and description of key performance aspects were presented. Role of each module as described and in later sections focus will be entirely on optimization of the heating chamber. The work presents an attempt of realizing divide and conquer principle, orthogonalize VLM into modules so that each module could be independently optimized for overall performance enhancement. Proof of correct orthogonalization is self-evident in the final experimental tests, as whether it was done correctly will be revealed from overall performance of the VLM which would be described in detail in Chapter 5. In a short summary, it could be observed that direction towards optimizing heater section should be done towards enhancing heat transfer to raise the temperature of the liquid to increase  $I_{sp}$  and make sure that heater geometry doesn't cause a reduction in pressure as thrust is a function of pressure only. This is the main objective and the greatest challenge of the project as efforts dedicated in that direction are challenging computation-wise and evolves study of highly complex physical phenomena linked together. Numerous analytical solutions made for specific geometry of heating structures (heat sinks, vaporizers, etc) are not directly suitable for integration in the VLM heating chamber. Moreover, the golden spot between pressure drop and heating efficiency needs to be determined as optimizing both at the same time is almost impossible.

# 2 | DESIGN APPROACH

*"All heat are the same"*

---

**Max Planck**

Among modules of the VLM presented in the previous Chapter 1, heating chamber is expanded in this Chapter 2. Parameters affecting the performance would be identified and design proposal will be motivated by the effect on key performance attributes. As a result of the performance evaluation design of the heating chamber will be presented with the justification of design choices. Thesis objective set will be studied to achieve these goals. Analysis of the chamber will be performed in two different sections "External Heat source" and "Internal Chanel geometry". Thus two main blocks of the heating chamber responsible for power generation and distributing it successfully to the water and surrounding. Each section has its own set of challenges and for ease of analysis, it will be studied one by one.

## 2.1 CONCEPT AND THEORY

### 2.1.1 External DC heat source

The source of the energy generating heat is a resistive element dissipating electrical power by thermal means. The magnitude of ohmic power could be expressed by well-known power equation 2.1:

$$P = IV = I^2R = \frac{V^2}{R} \quad (2.1)$$

Electrical behavior of the resistor is the primary point of information when making judgments about thermal phenomenons taking place in the VLM. Therefore, a resistor has to be precisely characterized and its behavior for the conditions it will be exposed under operation has to be well known. Stability and repeatability of the resistive response as well as operation range (limited by Melting Point (MP), pressure,etc.) is a point of concern.

Attribute	RTD	Thermocouple	Thermistor	Silicon IC
Temperature	-200 - MP	-200 -1200C	-55 -150C	-55 -125C
Linearity	Excellent	Fair	Poor	Good
Precision	Excellent	Fair	Poor	Fair
Response	Fast	Fast	Moderate	Slow
Cost	Moderate	Low	Low	Moderate
Packaging	Many	Many	Many	Limited

**Table 2.1:** Table with major attributes of temperature detecting methods [9]. RTD was chosen due to large temperature range and quick thermal response compared to other measuring methods.

### Resistor Characterization

Purpose of the heater for VLM application is not only generating heat but also deliver accurate information about power conversions taking place. In other words to serve as RTD. An RTD could be measured more accurately with a constant current method while the other methods (voltage divider, oscillator) also could be used. The benefit of a constant current method is the fact that change in resistance is measured only for the specific part of the resistor without taking into account parasitic resistance of the connection lines. No matter which method is used to measure, material property Temperature Coefficient of Resistance (TCR) ( $\alpha$ ) is a decisive quality of resistor affecting both sensitivity and accuracy of the readout. For an arbitrary resistive element with given shape resistance could be expressed as in equation 2.2:

$$R = \frac{\rho}{th} \frac{L}{W} = R_{sheet} \frac{L}{W} \quad (2.2)$$

Where:

$\rho$  - resistivity at room temperature [ $\Omega m$ ]

$L$  - Length [ $m$ ]

$W$  - Width [ $m$ ]

$th$  - thickness [ $m$ ]

$R_{sheet} = \frac{\rho}{th}$  - sheet resistance [ $\frac{\Omega}{\square}$ ]

Resistance described above is subject to change as a function of temperature, by detecting thus change temperature could be found. For temperatures below 100 °C resistivity could be expressed by first-order equation 2.3

$$R_t = R_0[1 + \alpha(t - t_0)] \quad (2.3)$$

When the temperature rises it might be useful to compensate the non-linearity in resistance change with necessary precautions of expressing resistivity curve with 3rd order Callendar van Dusen equation 2.4.

$$R_t = R_0[1 + At + Bt^2 + C(t - 100)t^3] \quad (2.4)$$

Where:

$R_t$  = resistance at room temperature [ $\Omega$ ]

$R_0$  = resistance at calibration temperature  $t_0$  in our case 0°C

$t$  = temperature [°C]

Material /Parameter (MP)	Thermal Conductivity [ $Wm^{-1}K^{-1}$ ]	Thermal Capacity [ $JKg^{-1}K^{-1}$ ]	Thermal Expansion [ $10^{-6}K^{-1}$ ]	TCR [ $^{\circ}C^{-1}$ ]
Mo 2896K	139.0	250	4.8	0.00460
Pt 2041.4K	71.6	133	8.8	0.00392
Ti 1941K	21.9	540	8.6	0.00380

**Table 2.2:** Several important material parameters suitable of serving as a heater/RTD

$\alpha$  = temperature coefficient of resistance [ $^{\circ}C^{-1}$ ]

A,B,C = coefficients that needs to be found for each resistor separately.

From equations (2.2 - 2.3) important RTD/Heater design parameters are initial resistance and TCR by which material choice is made. Summary of properties affecting a RTD for various materials are listed in the table 2.2. Stability of the performance in the long term is also crucial for the final product as the lifetime of the heaters should go beyond the testing stage. However, reliability tests like temperature & pressure stress tests or cycling tests to determine long term stability would not be performed.

What is equally important for both heater and RTD is the range of temperature it can go and preferably preserve linear output. Molybdenum was chosen due to its high MP and high TCR as well as its linearity over wide range [21] which exceeds widely used platinum RTDs.

#### 2.1.2 Internal Channel Structure

Joule heat generated by an external heater is delivered to the propellant through internal channel walls. The geometry of the walls plays a crucial role in terms of determining performance and stability. The heat removed by the propellant and pressure losses is directly dependent on the geometry of the fin structure. In addition to it, manufacturability and fluid mixing properties of the chamber are also a function of fin geometry. Therefore it was attempted to invest the effort to find a heater shape which could improve heat transfer and deliver the heat in a more uniform manner, as well as minimize pressure losses.

Many researchers tried to find optimal geometry for maximum heat transfer and conducted experiments by measuring heat transfer to the fluid through different geometries: results are shown in figure 2.1. In most simple terms the heat transfer coefficient to the fluid could be described by its properties and empirically determined constants. (equation 2.5)

$$Nu_d = CRe_d^m Pr^n \quad (2.5)$$

Here C,m,n - are constants determined empirically.

While, pressure drop could be expressed by equation 2.6.

$$\Delta p = f \frac{2L}{G^2} \frac{\rho}{D_h} \quad (2.6)$$

Where:

$f$  - Friction factor

$L$  - Length

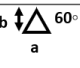
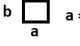

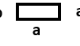

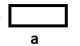
Geometry	Nusselt number at constant wall temperature	Product of f and Re based on hydraulic diameter
 $60^\circ$	2.47	13.333
 $a = b$	2.976	14.227
	3.34	15.054
 $a = 2b$	3.391	15.548
	3.657	16.000
 $a = 4b$	4.44	18.23

Figure 2.1: Average Nusselt's Number under constant wall temperature and product of friction factor & Re based on hydraulic diameter [30]

$D_h$  - Hydraulic Diameter of the channel

$G$  - Mass flux

$\rho$  - Liquid density

However, placing specific geometric structures in a channel doesn't necessarily reveal maximization of heat delivery. Study on the positioning of periodic structures inside the channel and their effect on friction factor and heat transfer were studied by [11] and summary of the results are presented in figure 2.2. Another, type of channel structure could be seen from the study of the [19]. Where straight ducts were compared to channel with periodic expansion and contraction. Results prove that periodic structure where fluid face contraction and expansion is indeed quite interesting and promising. Results of the study could be viewed from the figure 2.3. From study [11] and [19] it could be concluded that convection resistance decrease in a type of channel was fluid is exposed to expansion and contraction along its path to the exit. In addition to it, the positioning of the periodic structures plays an even more important role in heat transfer maximization, but it comes with pressure drop. Exact calculation of heat transfer in fluids comes along with computational challenges as analytic solutions doesn't exist in most instances. Therefore heat transfer and pressure drop inside microchannels are computed numerically, governing equations for 2-D analysis under the assumption of energy conservation and laminar flow are expressed in equations 2.17 - 2.18:

Continuity:

$$\frac{\delta u}{\delta x} + \frac{\delta v}{\delta y} = 0 \quad (2.7)$$

x momentum:

$$u \frac{\delta u}{\delta x} + v \frac{\delta v}{\delta y} = -\frac{\delta p}{\rho \delta x} + \nu \left( \frac{\delta^2 u}{\delta x^2} + \frac{\delta^2 u}{\delta y^2} \right) \quad (2.8)$$

y momentum:

$$u \frac{\delta u}{\delta x} + v \frac{\delta v}{\delta y} = -\frac{\delta p}{\rho \delta y} + \nu \left( \frac{\delta^2 v}{\delta x^2} + \frac{\delta^2 v}{\delta y^2} \right) \quad (2.9)$$

and Energy conservation criteria:

$$u \frac{\delta T}{\delta x} + v \frac{\delta T}{\delta y} = \psi \left( \frac{\delta^2 T}{\delta x^2} + \frac{\delta^2 T}{\delta y^2} \right) \quad (2.10)$$

Here:

$u, v$  - is directional velocity

$\psi$  - is liquid thermal diffusivity

$p$  - is pressure

#### *Understanding Heat transfer modes*

Energy generated by external resistive heat generated would be transferred through three modes: conduction, convection, radiation. Knowing exact quantities of each heat transfer mode will allow extracting important information about the heating chamber, which will allow determining water temperature and consequently characterize the performance of the VLM analytically as it was done in [7]. Moreover, it will be useful in the design of the external heaters as well as it could be seen from [13]. It is not possible to characterize the external heater without power management.

Heat Flux delivered to the propellant and dissipated to the ambient through convection and radiation is therefore summarized by equations 2.11 - 2.14:

$$Q_{water} = hA\Delta T_{wf} \quad (2.11)$$

$$Q_{rad} = \sigma \epsilon A (T_w^4 - T_\infty^4) \quad (2.12)$$

$$Q_{air} = h_{air} A \Delta T_{wa} \quad (2.13)$$

$$Q_{cond} = k \Delta T \quad (2.14)$$

Here:

$T_a$  - is ambient temperature

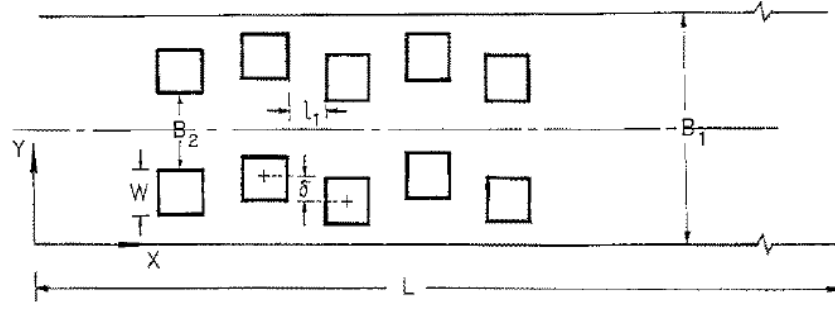
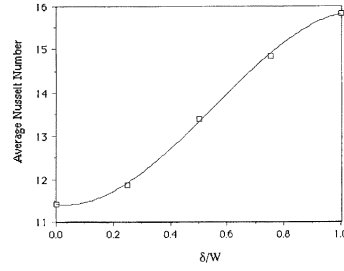
$T_w$  - is wall temperature

$T_f$  - is fluid temperature

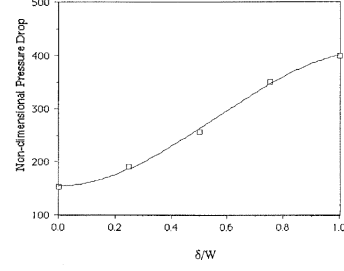
$\Delta T$  - Temperature difference within wall

#### *Equivalent wall temperature Interpretation*

One of the confusion arises when it comes to characterizing wall temperature whether to deal with non-uniformity or not. To keep things simple equivalent wall temperature will be taken as  $T_w$  for power estimations but clearly, the temperature difference is essential for electrical heat to reach propellant by the matter between them through conduction. The water temperature is also highly non-uniform through ought the heating chamber and simplification will be imposed in this instance as well. In literature, several ways of expressing equivalent liquid temperature are used. Equations

(a) Staggered fin structure dimensions ( $\delta$  - pitch size)

(b) Average Nusselt's number



(c) Dimensionless pressure drop

Figure 2.2: Heat transfer and pressure drop across staggered row structures ( $Re = 500$ ) as described by [11]

2.15 - 2.16 describes some examples found in the literature to describe the temperature difference between wall and propellant. Average temperature difference between wall and fluid:

$$\Delta T_{wf} = T_w - \frac{T_{fin} - T_{fout}}{2} \quad (2.15)$$

Log mean temperature difference as described in [15] is also used:

$$\Delta T_{wf} = \frac{(T_w - T_{fin})(T_w - T_{fout})}{\ln \frac{T_w - T_{fin}}{T_w - T_{fout}}} \quad (2.16)$$

When numerical simulations are conducted temperature distribution field can be calculated and one of this method could be used to interpret the result.

### 2.1.3 Power Consumption Estimates

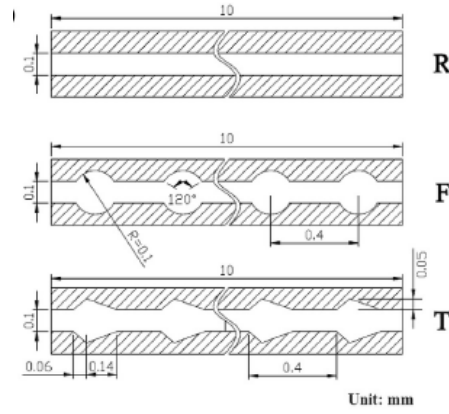
First of all for a given flow rate minimal power that needs to be applied to reach a point of vaporization and further increase the liquid temperature is determined by the following equations 2.17 - 2.19.

$$Q_1 = \dot{m}c_p(100C^0 - T_i) = \dot{m}c_p\Delta T \quad (2.17)$$

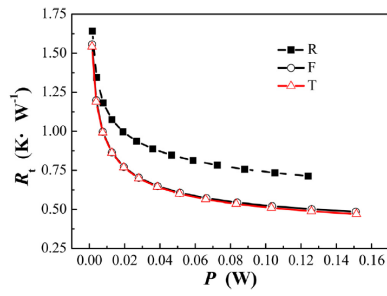
$$Q_2 = \dot{m}L_v \quad (2.18)$$

$$Q_3 = \dot{m}c_v(T_f - 100C^0) = \dot{m}c_v\Delta T^* \quad (2.19)$$

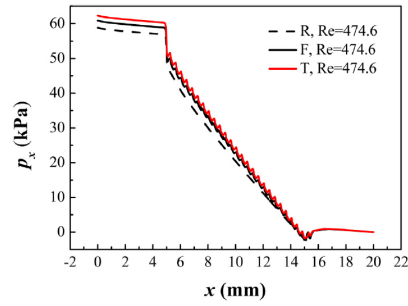




(a) Channel with periodic structure ( $\delta$  - pitch size)



(b) Thermal resistance of the channels



(c) Pressure drop

Figure 2.3: Heat transfer and pressure drop across periodic channel ( $Re = 474.6$ ) as described by [19]

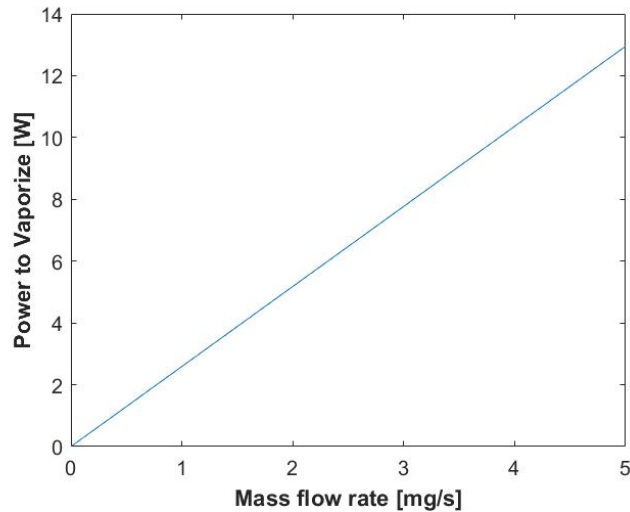


Figure 2.4: Minimal Power to Reach vaporization for a given flow rate [mg/s]

Where:

$T_i, T_f$  - initial and final temperature of the liquid

$L_v$  - latent heat of vaporization [J/kg]

$c_{p,v}$  - specific heat [J/kgC]

From figure 2.4 power needed for vaporization versus flow rate is shown. This basic information gives an idea about minimum power needs to be delivered for the system for the given mass flow rate range of liquid propellant. Which means convective heat flux 2.11 needs to be sufficient to evaporate the liquid.

It has to be noted that obvious disadvantage of the water as a propellant is its massive latent heat of vaporization, requiring a large amount of energy for achieving gas as an output. However, it is an advantage when it comes to multiphase cooling loop, where absorption of a large chunk of heat by a small volume of liquid is an important quality.

## 2.2 DESIGN RESTRICTIONS (REQUIREMENTS)

Overall, design choices are made with reliance on the conditions listed below. Although, they are separated into sections design requirements overlay and listed design conditions are not necessarily fixed. However, the design goal was tightened by thus requirements and they were used as the main guideline and partial and/or complete satisfactory of thus demands were conditioned in every step taken.

<b>Performance</b>	1. Effective Heat Transfer (Power Efficiency)
	2. Minimal Pressure Drop
<b>Manufacturability</b>	3. Compact Design
	4. Process Robustness
<b>Reliability</b>	5. Mechanical Sturdiness (Durability)
	6. Heater Stability
<b>Cost</b>	7. Power Efficiency
	8. Durability

More specific Design Requirements as given by [5] could be found in the Appendix A:

## 2.3 DESIGN PROPOSAL (VLM ARCHITECTURE)

As a summary of studies design conclusion had to be made. In order to do so, based on heat transfer modes thermal resistive network was constructed where thermal resistance is defined as in equation 2.20. This would allow determining heat transfer in steady state conditions.

$$R_{th} = \frac{\Delta T}{P} \quad (2.20)$$

Where  $P$  is power dissipated by one of the heat transfer modes. The more exact definition is presented in the next chapter of model verification. The basic principle behind the design was to understand the heating chamber as a resistive network and maximize the thermal resistance to the surrounding and minimize the path to the water. As for the geometry of convection, it is quite difficult to come up with a guaranteed working structure due to the extreme challenge of computational efforts it would require. However, thus arguments supporting design has to be tested.

1. Possibility to isolate (increase thermal resistance) heater from surrounding and within the VLM itself to deliver more heat to the propellant.
2. Will such a design offer compact and isothermal/stable solution?
3. Is it possible to achieve less pressure reductions?
4. Is it open doors for more accurate and fast temperature measurement.

Resistive network (figure 2.6) has its disadvantage, forced convective heat transfer coefficient cannot be determined, as such a design was never fabricated and tested. However, all the other heat transfer modes could be managed and independent of forced convection optimized. For convection to water all we could do without supercomputers is to try and test. In the next chapter result of thermal optimization would be presented.

### *Conduction Resistance - Lateral*

The energy transport by means of the matter is an important part of understanding the performance of the VLM. The thermal network figure 2.6 is a useful analogy for design optimization.  $R_{conductionlateral}$  conditions the transport of resistive heat generated by the heater in the lateral direction. It

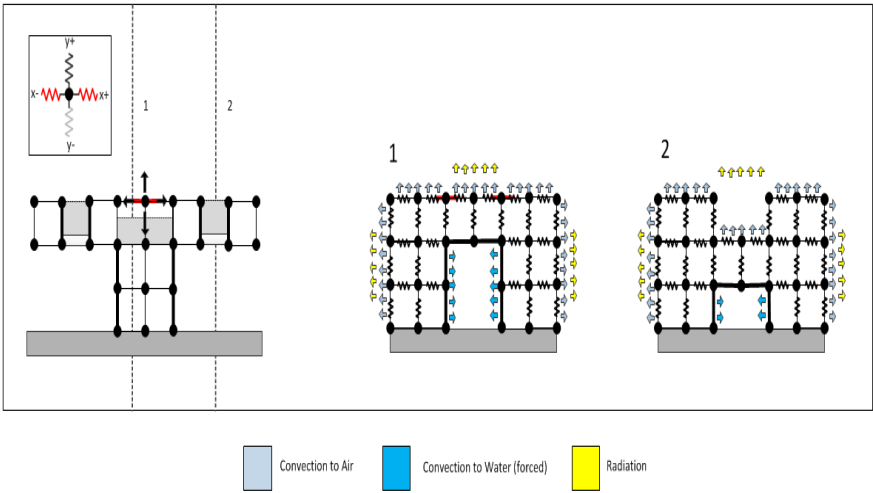


Figure 2.5: Design side view and cross sections

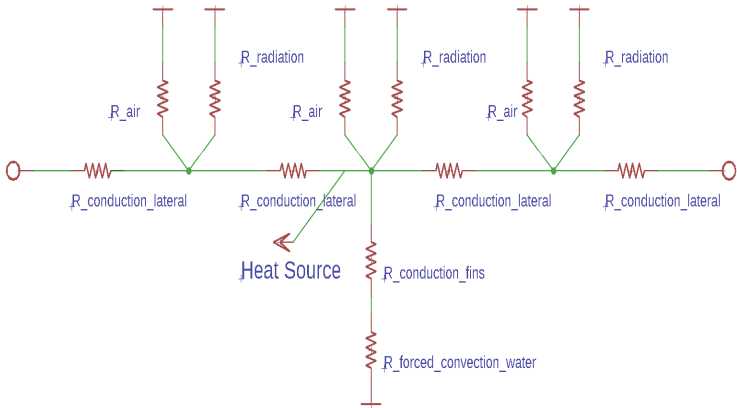


Figure 2.6: Thermal resistance network

is important to quantify the leakage and block the heat loss in that direction. One of the methods to do so is completely cut the silicon and remove matter in-between, however, this will create propellant leakage. One of the methods could be etching it till some depth creating thermal cavity like in [24]. This solution works if the pressure inside the channel is not extreme and has its mechanical sturdiness limitations. In another hand, if structure etched partially it still increase thermal resistance and keep mechanical strength. Etching pattern decides the structural strength and it was decided to etch it in right hexagonal shape ( $50\mu m$  side length) as honeycomb figure 2.9 with a depth of  $150\mu m$ . The result of calculation depending on depth could be seen from 2.7. If needed more aggressive silicon removal could be performed to achieve better results, but this should be done with consideration of pressure requirements. Another, more complex solution is to bond thermally insulating glass on top and create an island where the heater is located but with only access to interconnect wires. Thus, the concept would be presented in the summary Chapter 6.

$$R_{cond} = \frac{L}{kA} \quad (2.21)$$

Where:

k - thermal conductivity

L - length

A - area of contact

#### *Conduction Resistance - Fins*

With the same mindset, the conduction resistance to the fins was reduced by bringing it closer to the heater. In optimization of the conduction resistance, the only obstacle is fabrication limitations and pressure requirements conditioning mechanical sturdiness. This will also mean high aspect ratio channels as well as expansion and contraction of the liquid in its way which is a positive combination as it was discussed in this chapter. In this design fins were brought closer to the heater by making it deeper from  $100\mu m$  to  $250\mu m$ , therefore, keeping it only  $50\mu m$  away from the heaters placed on top.

#### *Convection Resistance - Air*

Convection resistance to air although not so critical for space application due to the absence of the air in the space. For earth conditions, it could be completely eliminated by capping or covering the heaters completely. However, variable seriously affecting it is heater width [13]. The wider the resistor more the resistance to the air.

#### *Convection Resistance - Water*

Channel geometry is the biggest challenge of the thesis and critical part of heater efficiency. However, the effect of fin geometry in straight ducts was already characterized by [33],[3]. It is not clear however how heat transfer coefficient will change in the double depth channel. Due to the little effect of gravity in microscale expansion and contraction in vertical direction should bring the same result as in lateral effectiveness of which was confirmed by

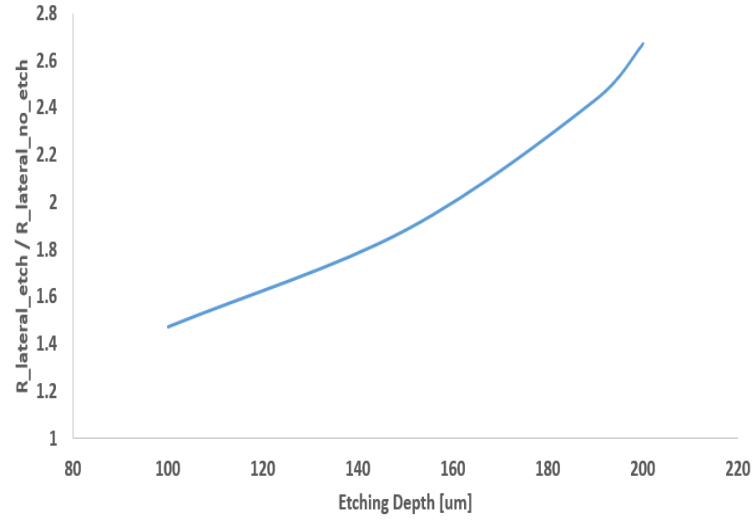


Figure 2.7: Rise of thermal resistance by etching hexagonal pattern.

[19]. In addition to it, the double depth channel represents from itself a larger surface of contact is perpendicular to flow direction at the exit of the channel which could balance uneven heat transfer.

#### Radiation Resistance

One of the parasitic effects from which power efficiency depends is loss of energy by means of radiation which is energy transport mode that doesn't necessarily need matter. The effect becomes dominant at higher temperatures and requires careful attention. However, a solution is relatively simple - appropriate packaging. Package of the VLM has to be constructed from a material with low surface emissivity at the outside and from the side looking at the heater it needs to be reflective.

##### 2.3.1 Uniformity

Uniform distribution of the heat generated by the heater is an important factor which cannot be overlooked. The precision of the measurements, as well as the lifetime of the device, primarily depends on the uniform heat distribution. Creation of hot spots deteriorates the part of the heater where it is generated as well as have a very negative effect on the performance of the VLM. As it was discussed in the previous chapter the heater instability might be, causing the local pressure drop and explosive bubbling. Therefore it was decided to put some effort into the uniform heat distribution of the VLM heater.

Design of the heating chamber was done in such a manner that each section of the heater is connected almost directly to the fin structure. The power generated in each section is subsequently removed by the water in a uniform manner. Therefore no significant hot spots are expected.

##### 2.3.2 Flow Instability Mitigation attempt

*Sputtering* effect according to leading experts in the study [36],[32] usually could be mitigated by either having sharp structures like diamond shaped

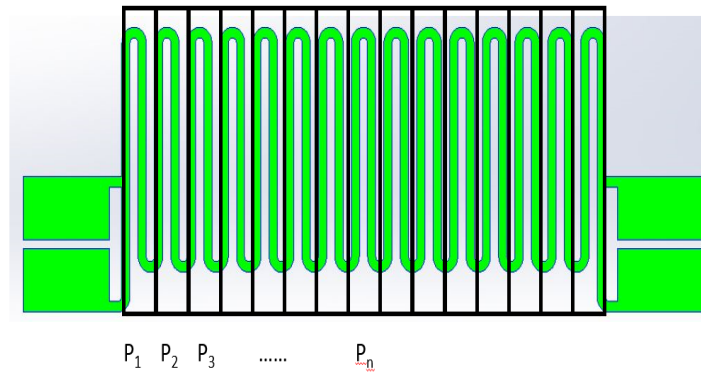
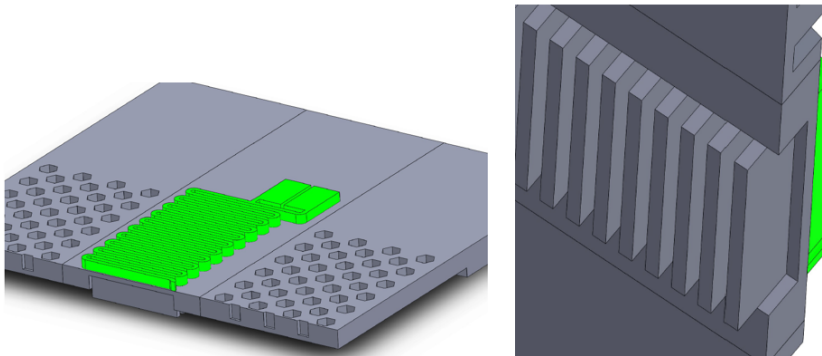


Figure 2.8: Illustration of uniformity achieved

or introducing pressure drop elements to elevate inlet pressure to suppress backflow. In this study, an attempt will be done on expanding the channel to offer flow expansion space along the direction of the flow and therefore elevate the inlet pressure to block the backward movement of the water. In addition to it, the structure will be adapted for pressure measurements for monitoring pressure oscillations by introducing physical access to the channel.



(a) Solidworks representation of the design cross section with necessary silicon bulk removal

Figure 2.9: Design representation

## 2.4 CHAPTER SUMMARY

As a result of the analysis of studies conducted in the past on microfluidic structures, it was concluded to experiment on various shapes and structures. Mathematically concluding best shape requires extreme computational effort and it is a task for fundamental fluid dynamic researches. Instead, various shapes with the best prediction based on empirical results of the past literature were decided to test. The experimental result should reveal promising geometry to further enhance the important properties like heat transfer and pressure drop. Underling idea is to come up with building blocks of microfluidic structures characterized and ranked based on heat transfer and pressure losses. Figure 2.9 helps to visualize the concept. When structures are characterized it is possible to organize them in such an order so that less efficient heaters are placed in front and more efficient ones towards back to balance the violent heat exchange at the inlet of the heaters due to the high-temperature difference. The concept of expansion and contraction would be applied in all direction. In other words, part of the channel structure would be deeper in some parts rather than others. Deeper in the places where external DC heaters are placed. This would reduce conduction resistance to deliver heat to the propellant. In order to reduce heat leakage, Si bulk was etched from the surrounding and therefore isolating heater. High aspect ratio channels etched below heater will also increase the surface of contact with the propellant and therefore it is expected that we should see an increase in heat delivery efficiency. External heat sources and channel geometries designed for this specific application is presented in the Appendix C and from now on each heater and channel would be mentioned by the index shown in the appendix.



# 3

## MODEL VERIFICATION

*"The strongest of all warriors are time and patience"*

---

**Tolstoy**

In order to verify the efficiency of the high aspect ratio fin structures, simple finite element simulations were done on COMSOL Multiphysics [1] software. To keep computation time manageable it was decided to use single physics domain of "Heat Transfer" without the coupling of "Electricity", "Laminar flow" and "Solid Mechanics". Conventional fin structure along with high aspect ratio was tested for their ability to deliver Ohmic heat generated from resistive source to the liquid. This knowledge will allow to estimate early predictions of expected efficiency and provide valuable data about trends performance tends to follow.

### 3.1 GEOMETRY AND MESHING

The basic principle of computation is solving equations conditioned by continuity laws. Therefore, in 3D simulations and in any simulation, in general, it is quite important to set basic building blocks properly so that simulation performed is accurate. In addition to it, element size determines a computation time and having a proper balance between calculation time and accuracy is essential. For this computation, CH2 was chosen and meshing which was used is a combination of a free triangular and free tetrahedral mesh. Minimum element quality set for simulation is 0.14. Digital model of micromachined silicon structure is shown in 3.1:

*Geometry of the heater which was used for running the simulation. The model was made according to the realistic structure which would be fabricated on 300 $\mu\text{m}$  thin silicon wafer bonded with Pyrex glass from the bottom. To test the efficiency of high aspect ratio fins two models of same CH2 type would be tested with the only difference of fin height which is 100 $\mu\text{m}$  for conventional and 250 $\mu\text{m}$  for high aspect ratio ones. Both structures have same channel depths of 100 $\mu\text{m}$ .*

### 3.2 BOUNDARY CONDITIONS

Setting boundary conditions properly are the most important element in simulation as the adequacy of simulation results will depend on it. The computation was executed by setting continuity condition and energy conservation law. All known heat transfer modes were identified and depending on the exposed surface the effect was taken into account in the simulation. As a result, expected heat removed by the environment and delivered to the

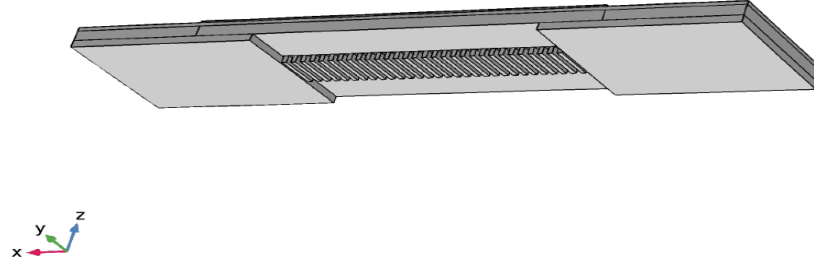


Figure 3.1: Digital model of the device

liquid was calculated. This was done for both high aspect and conventional fin structures and a difference in performance was a point of interest.

1. The sealed channel structures are subject to forced convective heat removal on the surface of contact with water. Although, heat transfer coefficient is a function rather than a constant for the thesis work equivalent value over the surface determined empirically will be taken. For the simulation, however, computation will be performed for some range of possible values of the convective heat transfer coefficient. Equation 3.1 shows the energy flux from the surface exposed to liquid.

$$Q_{water} = h(T_{wall} - T_{fluid}) = h\Delta T_{wf} \quad (3.1)$$

2. Top of the heaters are exposed to the air and heat is removed by natural convection. Equation 3.2 describes heat removal from the top surface.

$$Q_{air} = h_{air}(T_{wall} - T_{air}) = h_{air}\Delta T_{wa} \quad (3.2)$$

3. One more mode of heat transfer is radiation which can occur without the absence of matter. The relation of the energy flux from the surface radiating energy is described by equation 3.3.

$$Q_{rad} = \sigma\epsilon(T_w^4 - T_\infty^4) \quad (3.3)$$

4. The third mode of heat transfer as described by Fourier law 3.4 is conduction. The heat generated by the heaters is distributed by highly thermally conductive silicon bulk.

$$Q_{conduction} = k\Delta T \quad (3.4)$$

Net flux across the surface of the cube has to be zero according to energy conservation law, which could be seen from equation 3.5

$$Q_{\hat{x}+} + Q_{\hat{x}-} + \dots + Q_{\hat{z}+} + Q_{\hat{z}-} = \sum Q_{xyz} = 0 \quad (3.5)$$

After executing the computation it is possible to distinguish which mode of heat transfer were removing most energy. This is vital information in

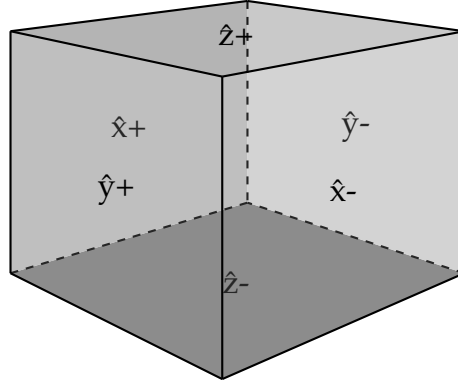


Figure 3.2: Cumulative flux of energy through all faces of the single element has to equal to zero

determining the efficiency of the overall system and in the calculation of the temperature of the liquid as well as in characterizing the performance overall. Representation of equation 3.5 in terms of heat transfer modes is presented in equation 3.6

$$\sum Q_{conduction} + \sum Q_{air} + \sum Q_{water} + \sum Q_{rad} = \sum Q_{Generated} \quad (3.6)$$

While this will also allow calculating thermal efficiency of the system overall as described before in 1.9 Expressing it one more time would be:

$$ThermalEfficiency = \frac{\sum P_{water}}{\sum P_{conduction} + \sum P_{air} + \sum P_{water} + \sum P_{rad}} \quad (3.7)$$

Precisely determined power delivery would allow quite accurate prediction of equivalent liquid temperature, for temperature distribution more complex coupling of flow dynamics with heat transfer modes needs to be accomplished but it goes out of the scope of the project.

#### Simulation Method

Generated matrices were computed by the Newton-Raphson method of linearization which in principle could be performed with other methods as well. For instance, the Gauss-Seidel method for this relatively simple simulation works as well.

### 3.3 DATA GENERATED

Once simulation conditions were set and definitions were given the remaining issue are material properties which are sometimes quite challenging to determine and values which need to be determined empirically (like heat transfer coefficient). As mono-crystalline silicon is well-studied material emissivity and thermal conductivity constants were taken from literature which is very reliable. However, the heat transfer coefficient to the air and

Element Surface/Condition	$\hat{z}+$	$\hat{z}-$	$\hat{x}+$	$\hat{x}-$	$\hat{y}+$	$\hat{y}-$
1. Top Surface	2,3	4	4	4	4	4
2. Right External Wall	4	4	2,3	4	4	4
3. Left External Wall	4	4	4	2,3	4	4
4. Left Internal Wall	4	4	1	4	4	4
5. Right Internal Wall	4	4	4	1	4	4
6. Top Internal Wall	4	1	4	4	4	4
7. Bottom Surface	4	0	4	4	4	4
8. Inner Elements	4	4	4	4	4	4
9. Fin front surface	4	4	4	4	1	4
10. Fin back surface	4	4	4	4	4	1

**Table 3.1:** Boundary conditions for elements based on heat transfer equations 3.1 - 3.4 (0 is denoted for insulation bottom glass). Corner elements are computed in similar fashion. Given large number of elements the error introduced by corner elements are negligible. Nevertheless, they are taken into account. for meshing used for this particular simulation computation are performed based on normal direction to the surface.

water are the function of temperature, geometry and even depends on fluid properties. Therefore a range of possible values was chosen to predict the general mechanism of system performance. Wall temperature versus power inputted for a different type of fins could be viewed from the figures 3.3 and 3.4. The result shows that more heat is delivered to the water from high aspect ratio fins comparing to the ones from conventional heaters. In terms of numbers, the difference of power delivered to the propellant between different types of heaters could be seen from figure 4.2.

### 3.4 ELECTRA THERMAL MODEL

Based on simulation results it is possible to imitate the thermal behavior in an equivalent electrical circuit. This is, however, not an ideal model of the system behavior, rather approximation and visualization of trend system tend to take. In other words, thermal resistance could be understood as the temperature increase per applied input power. Expressions describing thermal resistance of each heat transfer mode could be viewed from equations 3.8 - 3.10.

$$R_{radiation} = \frac{(T_{surface} - T_{air})}{P_{radiation}} \quad (3.8)$$

$$R_{convectionwater} = \frac{(T_{wall-contact} - T_{water})}{P_{water}} \quad (3.9)$$

$$R_{convectionair} = \frac{(T_{surface} - T_{air})}{P_{air}} \quad (3.10)$$

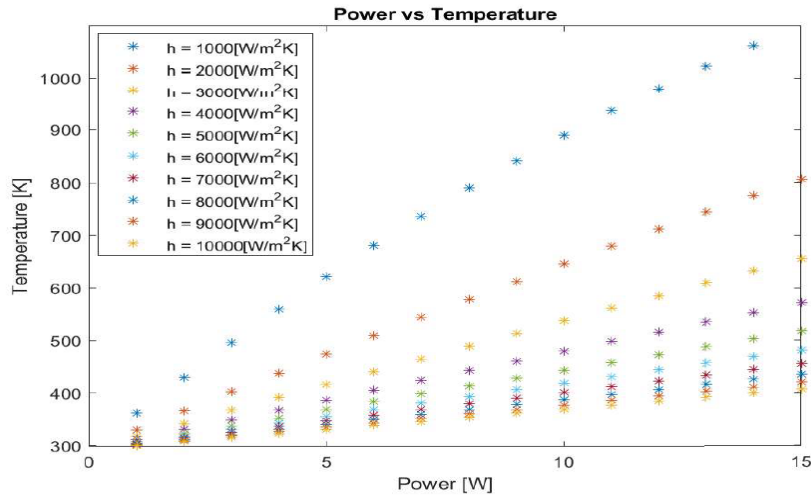


Figure 3.3: Power inputted to heat source and equivalent wall temperature of high aspect ratio fins.

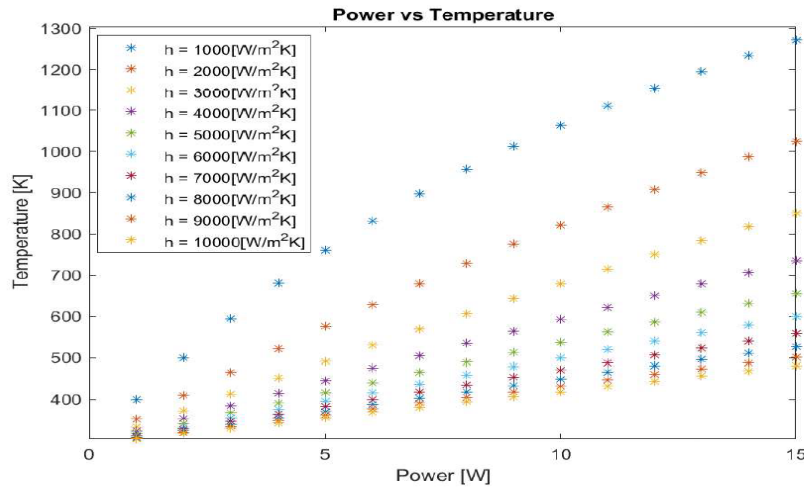


Figure 3.4: Power inputted to heat source and equivalent wall temperature of conventional fins.

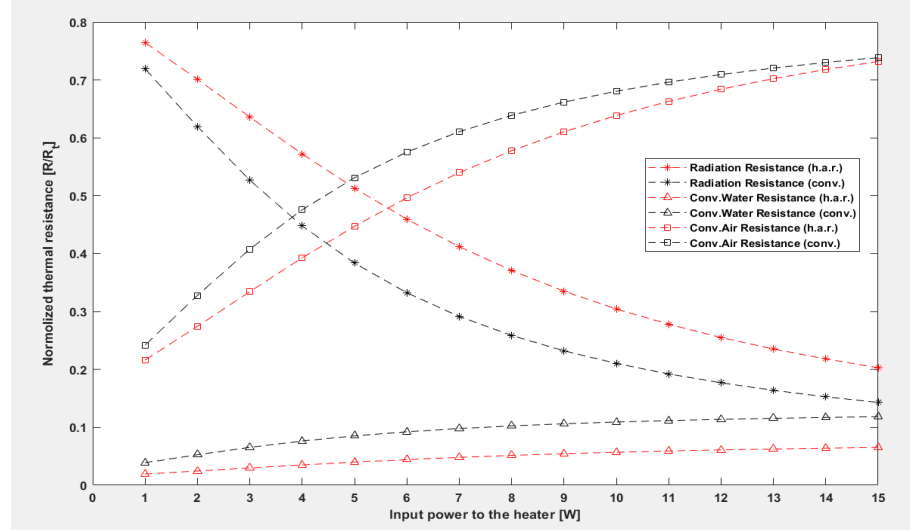


Figure 3.5: Normalized thermal resistance comparison

Where  $T_{surface}$  or  $T_{wall-contact}$  is equivalent (expected) temperature of the surface exposed to air and water. Its value is found by integrating the temperature of the surface overexposed area.

$$T_{surface} = \frac{\int T_{wall}(x, y, z) dA}{\int dA} \quad (3.11)$$

Graphical representation of thermal resistance could be viewed from figure 5.10 While, power delivered to the propellant for both type of fins could be derived from it by simple power equation.

*Normalized thermal resistance of conventional and high aspect ratio fin structures expressed over the range of [0:15]W input power at  $h_{air} = 100[W/(m^2K)]$  and  $h_{water} = 1000[W/(m^2K)]$ . It could be noticed that high aspect ratio fin structures have less thermal resistance to water, therefore delivers more power to the liquid.*

### 3.5 CHAPTER SUMMARY

In this chapter simulation results of conventional fins and ones with high aspect ratio were presented. Heat lost to the ambient as well as delivered to the propellant was computed for the range of heat transfer coefficient.<sup>1</sup> Results of the simulations suggest that high aspect ratio fins deliver more heat to the propellant under same conditions up to 20%. Thus, results were convincing enough to move into fabrication and test the outcome. Methods and assumptions in model verification computation are presented in detail. The main purpose of the simulation is not a fundamental fluid dynamics study but rather a more precise understanding of heater efficiency as well as use that knowledge for more accurate temperature monitoring. It has

<sup>1</sup> More advanced simulations using powerful CFD tool FLUENT will give a more comprehensive look at the structure and more reliable solution. However, simulations of 3D structures are extensive work and went beyond the timescale of the thesis.

to be mentioned that heat transfer coefficient to the water has very strong geometry dependence and if the difference for conventional and high aspect ratio heaters are not in our favor then only gain will be the reduction of conduction resistance. This, however, is still an improvement.





# 4 | FABRICATION

*"Only beautiful planes fly good."*

A. Tupolev

The detailed process flow for fabricating the device is attached in the Appendix B. This Chapter 4 discusses techniques used and challenges overcome to manufacture VLM. Although silicon IC technology is extremely advanced on parallel processing and on printing miniature components VLM is a 3-Dimensional device. Fabricating truly 3-Dimensional structures requires stretching silicon IC technology into extreme limits. However, advances in etching techniques open numerous opportunities to experiment with various structures which were not possible in the past.

**Quick overview of manufacturing techniques used in the fabrication of the VLM:**

**Lithography** - one of the main steps in any fabrication. Light sensitive organic material applied to the wafer and patterned through exposure to light. In this process, both positive and negative photoresist was used. A piece of equipment used in fabrication is ASML PAS5500/80.

**Sputtering** - a technique of depositing a specific layer on the flat substrate. Equipment used for this project is Trikon Sigma Magnetron.

**Wet Etching** - is etching technique where the desired layer is exposed to specific chemical and removed selectively without affecting other layers.

**Dry Etching** - or also known as (Reactive Ion Etching (RIE)) is an etching technique where ions are shoot to remove the specified layer. Equipment that was used for this procedure is: Drytek384 Triode & Trikon Omega

**Low Pressure Chemical Vapour Deposition (LPCVD)** - as the name suggests it is a deposition technique where a layer is deposited under low pressure. The disadvantage of the technique is its high thermal budget and therefore limiting its use only in the beginning of the manufacturing cycle.

**PECVD** - deposition technique where the desired layer is created underflow of specific gas and chemical reaction is enhanced with plasma.

**DRIE** - or also known as the Bosch process is an etching technique for creating much deeper structures on silicon comparing to other dry etching techniques. The process is accomplished by step-wise etching where in between steps polymer is applied to walls as protection. DRIE will be performed on the equipment - Rapier Omega i2L.

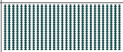
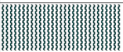
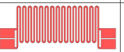


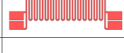

VLM MODULE	Bottom Layer (Channels)			Top Layer (Heaters)		
	Option 1	Option 2	Option N	Option 1	Option 2	Option N
Inlet				N/A	N/A	N/A
Channel/Heater 1		...			...	
Channel/Heater 2	⋮	⋮	⋮	⋮	⋮	⋮
	⋮	⋮	⋮	⋮	⋮	⋮
Channel/Heater N	⋮			⋮		
Nozzle				N/A	N/A	N/A

Figure 4.1: Visualization of the possible combinations which could be extracted by using modular design

**Anodic Bonding** - silicon wafer at the end of the process has to be enclosed by another wafer to seal the channels and serve as a mean of heat insulation. In this instance, anodic bonding is used. A method of joining silicon to glass wafers together to form one structure by aligning them together and applying high voltage and temperature. Under the influence of electric field Na ions are driven to the silicon surface and disassociated oxygen ions form permanent irreversible bonds with silicon. ( $\text{SiO}_2$ ). Glass to Silicon bonding will be performed on AML Bonder.

## 4.1 MODULAR FABRICATION

### *Advantages of Modular Fabrication*

Partitioning of the heating chamber and whole VLM could be viewed in Appendix D. This was done in order to be able to assemble VLM with varying characteristics. Various channels were exposed into the mask so that any combination and number of channels could be connected to reach desired characteristics (figure 4.1). In other words in modular design VLM resemble parts of Lego out of which numerous combinations could be extracted. This is very handy as in one satellite array of VLMs optimized for different performance attribute could be installed: one group build for thrust (minimum pressure drop) and one group for  $I_{sp}$  (maximum achievable temperature). In this project modular design allows us to test many combinations of heaters and channels and point out on variables affecting the performance most. Although virtually any combinations of channel structures could be fabricated, such a flexible design was chosen due to the necessity to explore various structures as it was mentioned before in Chapter 2. It is unfortunately not possible to simulate all the structures. In addition to it, such a design is more forgiving for uncertainties in the design. Several combinations of channel structures and heaters which together makes VLM could be viewed from the figure 4.2. Furthermore, the final goal of the DELFII mission is to integrate several modules of the VLM into one piece, where separately designed advanced modules are combined to boost the performance. The following design is made in blocks ready/suited for integration.

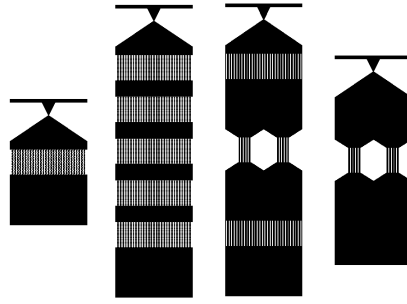


Figure 4.2: Several Example of what could be extracted using modular design while total combination could be extracted is virtually infinite

## 4.2 PROCESSING

### 4.2.1 Front side processing

Fabrication of the external heaters made from Molybdenum was accomplished by following numbered procedures below. Graphical representation of fabrication steps on double side polished  $300\mu\text{m}$  silicon wafer of P-type could be seen from 4.3. Example of heaters are widely available in the literature and similar devices could be seen from the works of [20] [21]. In our case, the design was modified to withstand high pressure from the propellant supply forcing the liquid to accelerate towards nozzle throat. An upper bound of the operating pressure of the VLM is approximately 5[bars]. Therefore, saving power consumption with making thin membrane is not possible and some amount of silicon bulk is left to preserve physical sturdiness to withstand pressure in the heating chamber.

1. Silicon dioxide ( $200\text{nm}$ ) is thermally grown to serve as passivation layer as well as to increase the adhesiveness of silicon nitride which will be performed in later steps. Thermally grown  $\text{SiO}_2$  layer could be used as a landing layer when backside DRIE will be performed. However, design of the VLM in order to keep structural strength will not include thin membranes as the pressure in the chamber is up to 5 [bars].
2. Low stress silicon nitride ( $500\text{nm}$ ) is deposited by LPCVD technique at  $850^\circ\text{C}$ . Although this step could be performed by PECVD as well it was reported by [20] [21] that LPCVD nitride shows better immunity to thermal stress rather than PECVD.
3. Molybdenum ( $100\text{nm}$ ) is deposited by sputtering in Trikon Sigma magnetron reactor. A layer of such thickness exhibits a sheet resistance of  $1\frac{\Omega}{\square}$ .
4. In order to protect Molybdenum which is vulnerable to oxidation beyond  $300^\circ\text{C}$  PECVD TEOS ( $300\text{nm}$ ) at  $350^\circ\text{C}$  is grown. PECVD TEOS layer would be also used as a hard mask to pattern Molybdenum.
5. Molybdenum is patterned by dry etching in Trikon Omega. Molybdenum, cannot be exposed to air for too long and needs a protective layer from the top.
6. Hard mask PECVD TEOS is removed by BHF solution and new layer ( $600\text{nm}$ ) of PECVD TEOS at  $350^\circ\text{C}$  is deposited.
7. Now in order to open pins PECVD TEOS is etched. First by dry etching followed by BHF wet etching. Two-step etching is done in order to remove all the oxide in pins.
8. Aluminum Layer with a thickness of ( $1\mu\text{m}$ ) is deposited by sputtering

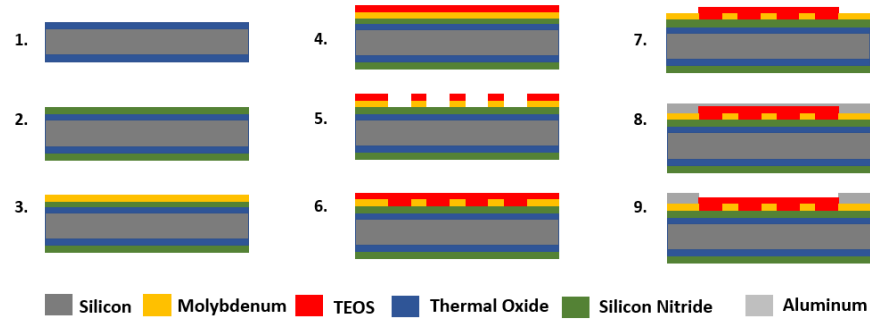


Figure 4.3: Process steps for front side fabrication

in Trikon Sigma magnetron reactor. Purpose of this layer is to improve the adhesiveness of Mo and gold wire bonds connecting heaters/RTDs to the external circuitry (PCB). However, Aluminium is not a good choice as a pad as it limits the operation range of VLM due to the low melting point of  $500^{\circ}\text{C}$ . For the future devices, more hard environment compatible material should be used to get full benefits of molybdenum heaters.

9. As the last step for front side - aluminum is patterned by dry etching in Trikon Omega.

#### 4.2.2 Back side Processing

Design Pattern of the channel is not uniform and there are sections which are deeper than other parts. Therefore, silicon has to be etched till several different depths, one going almost all the way through the whole wafer. In this instance, the standard procedure for DRIE with a single mask is not suitable. In literature, there are examples of etching silicon with several steps. For instance, four-step etching could be found in the work of [31]. Where combination/stack ( $\text{SiO}_2$ , Al, Photo Resist (PR), Al) of soft-hard masks were used. Such an approach allows to etch till certain depth and selectively remove layers of the mask and continue etching. In this work a similar approach was taken. In order to achieve structures with different depth silicon was etched from the front side and from backside creating double depth pattern in each side and meeting at some point creating a complete hole in silicon.

10. Procedure for the back side processing starts with the stripping of the oxide and nitride layers. Nitride layer and oxide layers are dry etched in Drytek. Thus, however, leaves remainings on the sides of the wafer in a ring-like shape. This is due to the imperfection of the machine which cannot etch sides of the wafer due to handling (cannot etch parts which are used to fix wafer in one position).

11. Now, hard mask PECVD TEOS ( $2\mu\text{m}$ ) is deposited at  $350^{\circ}\text{C}$ . Mask will protect parts of silicon from DRIE in later steps.

12. Photoresist (SPR - 3012) is applied and patterned to serve as a mask. Later, the surface of PECVD TEOS is patterned by dry etching. The photoresist is stripped and applied one more time (AZ-12-XT [18]) to serve as a soft mask for DRIE.

13. DRIE is performed on silicon to etch it up to a specific point. This is done to achieve deeper structures in the parts where external heaters are placed.

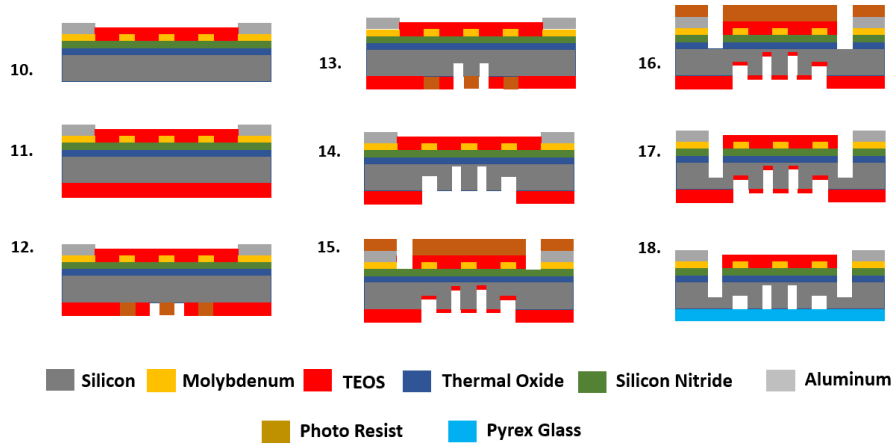


Figure 4.4: Process steps for back side fabrication

**14.** Photoresist is stripped and DRIE is resumed. Parts of silicon which were protected by soft mask this time is exposed into ion bombardment while already etched parts are etched further. As a result, a two-step structure is achieved.

**15.** Backside surface is cleaned and a layer of PECVD TEOS ( $1\mu m$ ) is applied as landing layer. While the front surface is coated and oxide, nitride layers are removed.

**16.** DRIE is performed from the front side and we land on the PECVD TEOS layer by which backside was covered. In this step, it has to be noted that DRIE was performed not only by using a soft mask (AZ-12-XT) but another hard mask layer in parts was shallow etching was required. This technique will be discussed more in-depth in a later section.

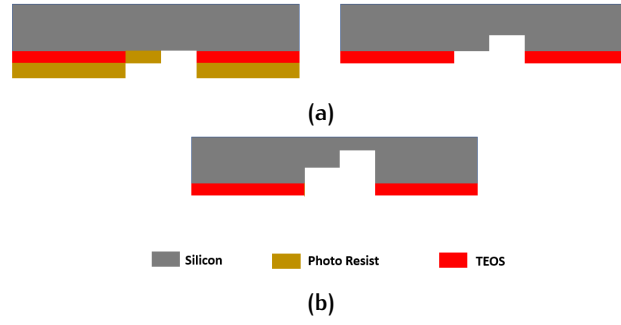
**17.** The PECVD TEOS layer is removed by wet etching in BHF (20minutes) from the backside and after etching photoresist is stripped from the front side.

**18.** Resulting structure is bonded into Pyrex Glass by anodic bonding technique. The process is performed in AML bonder at  $400C^0$  and at  $800V$  for  $15min$  or until  $2200mC$  charge is accumulated.

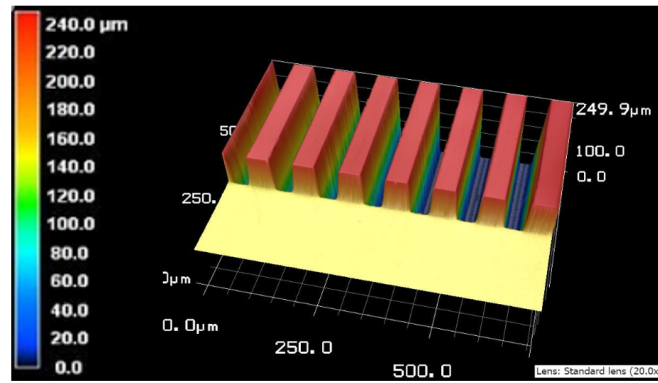
#### 4.2.3 Expansion on DRIE

##### *Backside double depth etching*

Design of the VLM required a decrease of thermal resistance and robust rise time of temperature for given input power to the heaters. This could be achieved by decreasing the silicon mass beneath and in surrounding areas of the heaters. Many conventional heaters use thus techniques to achieve  $[mW]$  region power for gas sensing with the quick response time. However, for the VLM design - the minimum power to reach vaporization of water for a given flow rate of  $1.6[mg/s]$  is  $5[W]$  therefore, the main element for power saving is packaging and for response time is efficient heat removal and reduction of the silicon mass. Advancements, in etching techniques like DRIE, is allowing to create complex shapes and structures which might enhance the heat transfer to the propellant and allow compact and robust design. Although the etching technique was covered in the previous section of processing it is explained in more in-depth in this section.



**Figure 4.5:** (a) Prepared hard mask PECVD TEOS ( $2\mu m$ ) and soft mask AZ-12-XT ( $10\mu m$ ) which is stripped after silicon is etched  $150\mu m$  (b) Resulting structure after additional  $100\mu m$  etch. The parts of silicon which were exposed to DRIE is etched up to  $250\mu m$  while parts were covered with photoresist is etched  $100\mu m$  (reference is bottom plane)



**Figure 4.6:** Keyence 3D microscope capture of the fin structure (backside of the wafer). Multiple step deepness could be observed where the deepest parts going all the way to  $250\mu m$

In order to create a step-wise structure in the silicon - two masks were prepared. The first mask is a PECVD TEOS thickness of  $2[\mu m]$  deposited on the silicon surface and patterned by dry etching. On top of it,  $10[\mu m]$  of AZ-12XT-20PL was applied by following instructions offered by the supplier [18]. A chemically amplified positive photoresist was patterned using  $120[mJ/cm^2]$  energy on the channel section right below heaters are placed. Thus allow us to DRIE etch thus section ahead of other section which will be etched and thus creating deeper channel structures. A visual explanation of the paragraph could be viewed from the figure 4.5. While the result is presented in figure 4.6.

#### *Front side double depth etching*

In order to connect VLM with a microfluidic interface and install pressure sensors inlet holes needs to be etched to have access to the channels. There also a need for silicon removal from the top to reduce leakage heat by means of conduction and later on dissipation by convection or radiation. The resulting structure designed for heat-trapping also decreases rise time and overall mass of the VLM. To achieve such structure similar to backside double depth etching technique was implemented by using several masks. However, for this procedure mask is not removed rather etched as well but with different

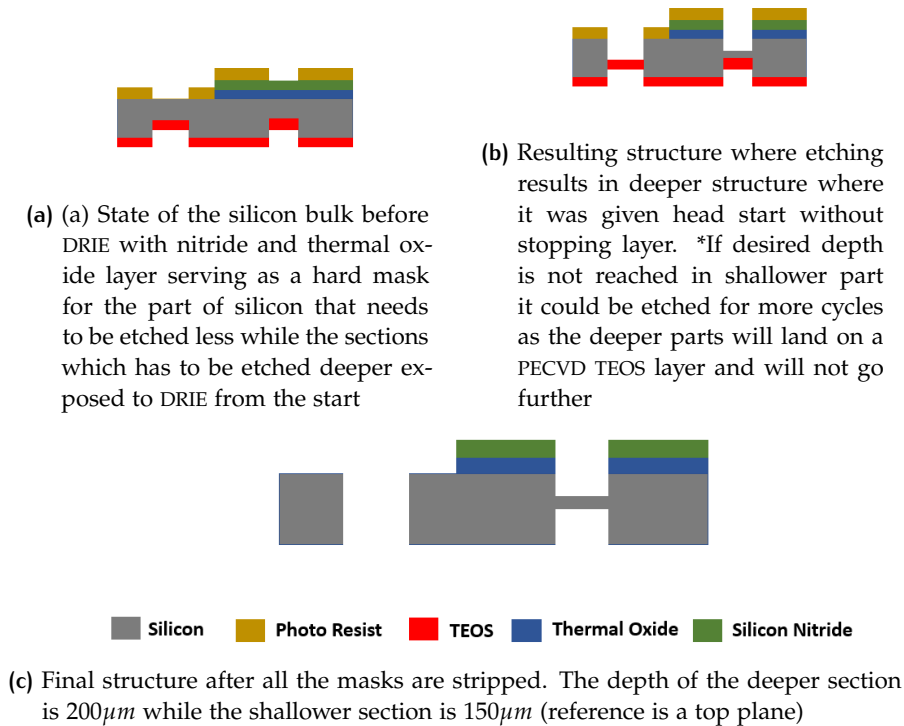


Figure 4.7: Front side DRIE processing procedure visualized

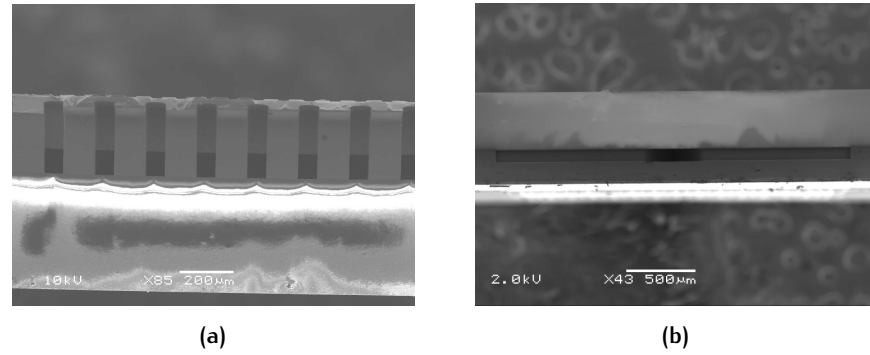
rate and as result structures with different depth are achieved. A figure representing the visual image could be seen from figure 4.7

#### 4.2.4 Anodic Bonding

Enclosing of etched channel structures is sealed with Pyrex Glass wafer. Bonding to glass is preferred over silicon to silicon bonding due to several crucial advantages. 1<sup>st</sup> it allows to visually observe the flow and determine flow regimes as well as observe phase change phenomena for more hand on interpretation of the heat exchange process. In addition to it, it reduces heat leakage as glass is an almost perfect insulator. Moreover, anodic bonding is a very strong bond which can withstand high pressure up to 10 [bar].

Silicon to silicon bonding in this case is not preferred as it was described in the processing section there was multiple oxide deposition used as a hard mask for DRIE and as an electrical passivation layer. Thus layers leave residual stress on the silicon which might influence bonding in a negative manner (cracks, improper bonding due to the deformed top wafer). In principle PECVD TEOS used as a hard mask could be avoided by using proper photoresist suitable to serve as of mask for plasma etching steps. However, materials used as a heater requires a passivation layer for electrical insulation and shielding layer protecting the metal from oxidation due to exposure to the air.

Pyrex glass has a similar thermal expansion coefficient as Si and more forgiving to defects as under high temperature it became more flexible and takes the shape of Si. However, oxide residuals need to be completely removed as it will create bonding failure (no bonding is possible with the



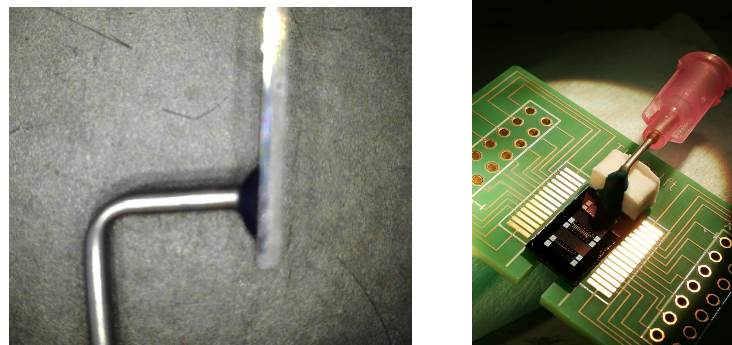
**Figure 4.8:** SEM capture of the chamber cross section and nozzle for quality evaluation

dioxide layer). SEM image of the heating chamber with bonded Pyrex glass from the bottom could be seen from figure 4.8.

#### 4.2.5 Connection to microfluidic interface

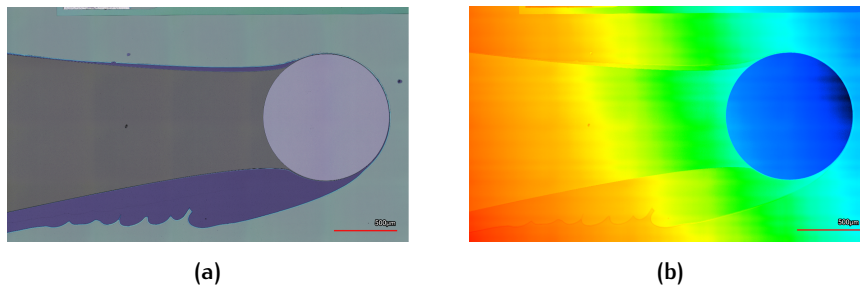
Inlet of the fabricated VLMs needs to be connected to the fluid source without any leakage and blocking the free movement of the propellant. For the experiment it will be done in a simple yet functional way of attaching the metal microfluidic tip by (ABLESTICK) glue. Curing it afterwards by high temperature ( $120^{\circ}\text{C}$ ) for 2 hours. Thus connections were tested by running the liquid at various pressure ranges and yet no leakage was observed. (figure 4.9) However, the resulting structure is not very sturdy and needs to be handled with great care.

High-temperature requirements applied for the materials of the VLM heater are not necessarily applicable for the microfluidic interface for testing purposes. The design of the chamber was accomplished in a way that heat is trapped only in the fin structures and there should be a large temperature difference between the inlet section and the heating chamber. This gives the flexibility of the material choices for realizing the microfluidic interface.



**Figure 4.9:** Side view of individual die connected to the microfluidic interface and attached to the PCB with the 3D printing support for more reliable handling





**Figure 4.10:** (a) SPR 3012 failure due to topography created after etching PECVD TEOS and Molybdenum inside inlet holes. This surface was prepared for later on DRIE etching. (b) Optical microscope capture of uneven surface created due to SPR 3012 failure. This was fixed with adjusting coating recipe by reducing (rpm) and therefore applying thicker resist.

#### 4.2.6 Challenges during Fabrication

##### ***Photo resist issue***

###### ***SPR-3012***

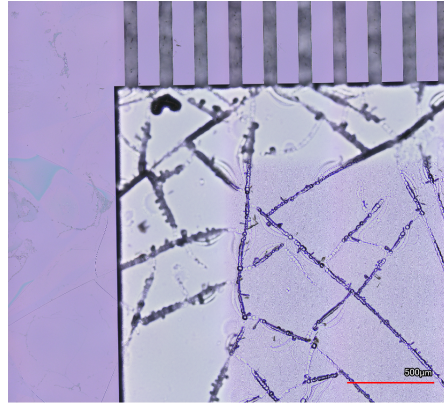
Topology created whether by dry or wet etching prevents the uniform distribution of the photo-resist during coating. For the front side mask for DRIE surface prepared from initial steps where deep inlet holes required removal of Molybdenum and other layers. Even though not significant some uneven topography was created. This resulted in the absence of photoresist behind inlet holes and later steps followed like PECVD TEOS etching resulted in unwanted etches. From figure 4.10 it could be seen how the absence of photoresist resulted in unwanted etch of the PECVD TEOS layer.

###### ***AZ-12-XT20PL***

Using the photoresist layer as a soft mask during DRIE, in general, worked out. However, it was also observed that in some instances photoresist was partially removed during DRIE which resulted in unwanted etches. It could be seen from figure 4.11 where it is visible, parts where the photoresist fell off resulted in a rough surface and unwanted holes. Hard mask beneath photoresist deposited with some reserve to withstand more than it takes to etch channels, therefore, photoresist failure in that parts are not point of concern. However, the question arises when photoresist fell off from the bare silicon surface resulting in roughness. This could potentially detriment performance of the VLM as well as make the device more fragile if the etches are deep.

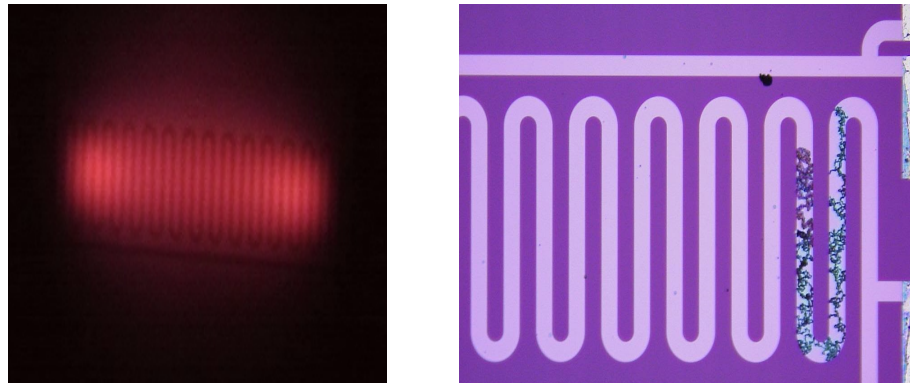
##### ***Molybdenum Oxidation***

It is a well-known fact that molybdenum oxidizes at the high temperatures once exposed to air. Therefore, a protective layer was deposited (see Front side processing). However, (600nm) of PECVD TEOS layer deposited as protection had relatively poor quality in terms of isolation. Later on in the experiment section it was observed that TEOS layer had small holes (*non-uniform deposition*) which were the reason for partial oxidation of the heaters which resulted in unwanted instability of resistance. Once they were heated up to large temperatures (more than 350C<sup>0</sup>) irrecoverable increase of the resistance was observed in some of the resistors. In some cases oxidation

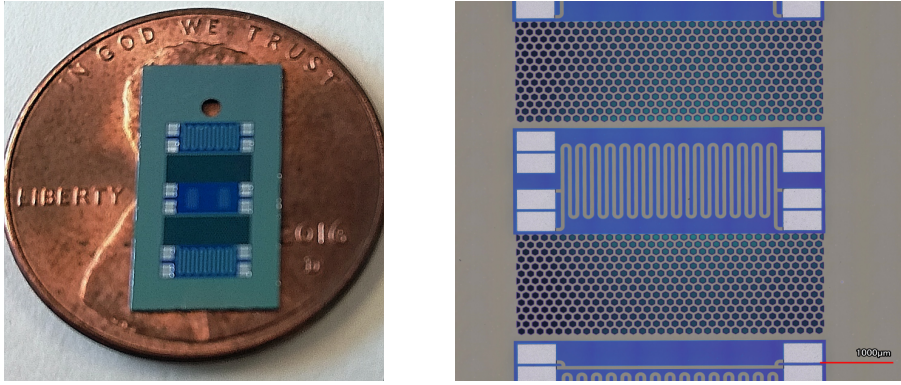


**Figure 4.11:** Keyence 3D microscope capture of roughness created after DRIE due to fall off of photoresist. This however was observed in several devices didn't spread to whole wafer. Reason for poor adhesiveness of the AZ-12-XT20PL photoresist could be the patterned PECVD TEOS layer(hard mask). Topography of which prevented good adhesiveness.

resulted in the complete destruction of the resistor. (see figure 4.12). Therefore, to guarantee the right functionality of the heaters another protective layer should be applied for future research: it could be SiC or SiN. Both of them are good candidates. Thermal conductivity of the SiC makes it suitable and desirable layer to serve as a heat spreader for uniform distribution of the heat across the heater surface as well as provide incredible sturdiness to the structure.



**Figure 4.12:** Oxidation happened after the heater was heated up to high temperature ( $600\text{C}^0$ ) this resulted in formation of hot spots as resistance at the high concentration of pinholes grew significantly



**Figure 4.13:** Front side picture of finished product, presented with a penny in the background (diameter of which is  $19.05\text{mm}$ ).

### 4.3 CHAPTER SUMMARY

In this Chapter 4 procedure for manufacturing the VLM was presented and the result of the work could be viewed from (figure 4.13). VLM fabricated using MEMS techniques is quite an elegant device which requires stretching planar IC fabricating methods into a more complex 3-Dimensional structure. Moreover, the challenge is added later on when handling the resulting fragile micromachined device and taking care of its reliable functioning along with the microfluidic interface. However, resulting structure is expected to be more advanced in functionality and applicable in many other fields to suit various purposes. During the fabrication <sup>1</sup> various step-wise DRIE etching methods were experimented and process of VLM fabrication was developed. This process could be used in the future and further developed for integration of all modules of MEMS VLM. The yield of the process was very high and most of the devices had a clear and sharp structure with desired dimensions, however, there were several minor issues which were discussed in the chapter. Thus issues were solved for the last set of devices fabricated: front side comets and DRIE roughness were removed by a better recipe of the manual coating.

<sup>1</sup> It has to be noted that EKL has excellent recipes for DRIE which allows fabricating very smooth channels. Although not discussed in the thesis surface roughness might alter performance in a negative way [3].



# 5

## CHARACTERIZATION

*"An experiment is a question which science poses to a Nature and a measurement is a recording of Nature's answer"*

Max Planck

### 5.1 EXPERIMENTAL SETUP

Testing and verification of power performance of the heating chamber will be done in several steps. First, the sheet resistance of the fabricated resistive elements is tested for resistivity uniformity and the effect of process variation. This will ensure that structures are functional and behaving as expected and nothing wrong or unexpected happened during fabrication. Later on, several wafer level measurements with an intention of determining resistance at room temperature and extract linear behavior of the RTD over the wide temperature range are performed. This experiment will require an environment with precise temperature control. In other words, RTD/Heaters are calibrated and their temperature behavior is documented. As a final stage thus information will be used to determine the thermal resistance of the channels by applying power and measuring temperature ratings. This procedure will be done for wafer level devices and for the final product as well as with liquid flow and without. Results should reveal if efforts done in realizing different structures for better heat removal are paid off. Experimental set up for each measurement performed is shown in figure 5.1.

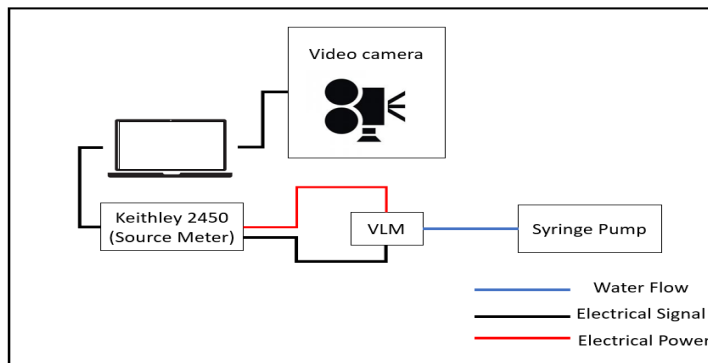
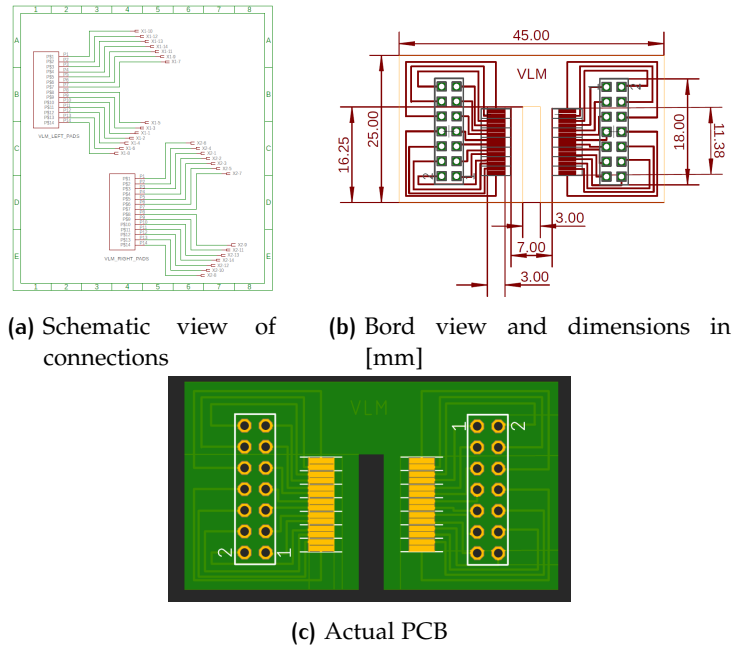


Figure 5.1: Experimental setup for the heater characterization

### PCB layout

To perform measurements VLM is mounted on PCB which is specifically designed for this application. It has  $3\text{mm}$  by  $16.250\text{mm}$  square window through which fluid motion could be monitored. Transparency of the VLM achieved by using a bottom wafer made of Pyrex glass made possible, visual observation. Fluid motion, as well as phase change phenomena, could provide very useful information about the performance of the heating chamber. Design of the PCB was made very simple and as compact as possible. The layout of the PCB could be viewed from the figure 5.2.



**Figure 5.2:** Pin assignment, dimensions and routing of the custom PCB designed for the VLM measurements. Design of the VLM includes Pyrex wafer as a bottom insulation and it is expected that it will serve as good insulation layer, removing any need for additional heat protecting measures in PCB design. Pins for VLM connections are made of Au as its suitable metal for wire bonding.

It has to be noted that PCB was good enough to withstand the heat flux generated by the heaters during the wet run (wall temperature up to  $500\text{C}^0$ ). However, such an attempt shouldn't be made without water as after some time the whole chip will be hot and eventually PCB will start to melt. Nevertheless, for operation regime bottom insulation by glass wafer showed very good heat-trapping quality. It will be a very good idea to do the same with the top surface, as for operation in pulsated mode needs very good thermal insulation for sustaining the heat generated.

## 5.2 ELECTRA – THERMAL CHARACTERIZATION

### 5.2.1 Process control – Sheet Resistance

Basic parameters of the RTDs/heaters like sheet resistance need to be pre-determined for the future temperature/power measurements and for the analysis of the results. This could be done by performing four-probe measurements on Vand der Pauw structures figure 5.1. For this purpose process control modules were placed in the wafer. The sheet resistance of the metallization layer (Molybdenum) was tested immediately after deposition and later on after fabrication of the full device was accomplished it was tested one more time to observe any variation from the initially determined values due to introduced conditions during manufacturing.

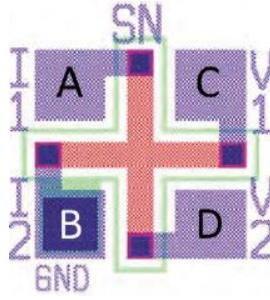


Figure 5.3: Van der Pauw structure

Sheet resistance is determined through equation 5.1 which includes a Vand der Pauw factor in front of determined resistance.

$$R_{sheet} = \frac{\pi}{\ln 2} R_{AB,CD} \quad (5.1)$$

Layer	Sheet resistance [ $\Omega/\square$ ]	Standard deviation
Molybdenum	0.9851 [ $\Omega/\square$ ]	10.85 [ $m\Omega/\square$ ]

Table 5.1: Table representing values of sheet resistance measured directly after metallization step

Uniformity of the layer doesn't cause concern as it could be seen from table 5.1 standard deviation is very small. The layer quality is an important parameter More detailed values are presented in the Appendix A.

### 5.2.2 Wafer level measurements for RTD calibration

Each heater/RTD fabricated was characterized by four probe constant current measurement under different temperatures figure 5.4. The experiment was done on CASCADE 33 probe station and on Au (gold) chuck which was heated up to  $200^{\circ}\text{C}$ . For each temperature step - measurements were paused (halted for 15min) so that the whole wafer could stabilize at the temperature set for the measurement. Starting from the room temperature of  $20^{\circ}\text{C}$  four-probe measurements were taken with a temperature step of  $25^{\circ}\text{C}$  till the maximum allowable  $200^{\circ}\text{C}$ . The purpose of the experiment was to characterize RTD or in other words calibrate its resistive response to temperature variation. Parameters like initial resistance at room temperature and  $\alpha$  - TCR need to be predetermined so that it could be used later on for temperature measurements. TCR determined for heaters were  $0.0025[^{\circ}\text{C}^{-1}]$ . In literature, however, almost twice as big values could be seen. The Mo TCR varies due to layer deposition quality, temperature, and some other process parameters. Therefore only a reliable mean of determining it is through empirical data collection as shown in figure 5.4.

Although, VLM's expected range of operation goes beyond  $200^{\circ}\text{C}$  for later

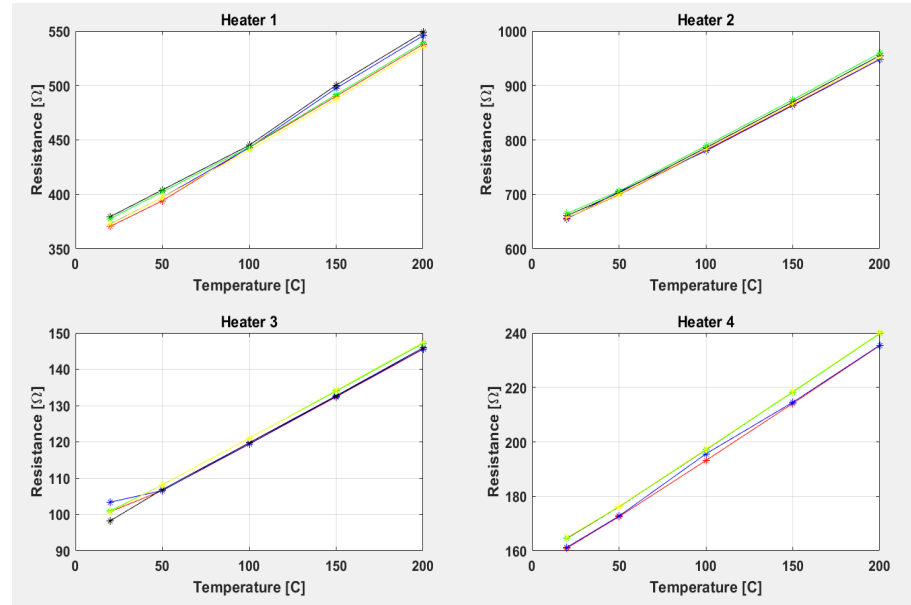


Figure 5.4: Calibration curve of all heaters (images of each heater could be viewed from Appendix A)

values linearity of Mo will be used to interpolate and predict the resistive response up to a maximum of  $500^{\circ}\text{C}$ . There gonna be some discrepancy with calibrated values and later on temperature measurements as during calibration gold chuck offers uniform heat while Joule heating results in higher heat loss in the sides [14]. As a result in later usage slightly higher temperature ratings are expected for temperature measurements.



### 5.2.3 Thermal Resistance

The thermal resistance of each channel could be described after external heaters RTDs were calibrated. Input power to the heaters should result in a rise of temperature. This information should reveal the expected efficiency of the device. Power delivered to the heaters are measured before the introduction of the water and after the specific flow rate is introduced to the VLM heating chamber. For the specific experiment, the radiation was neglected.

#### *Dry run*

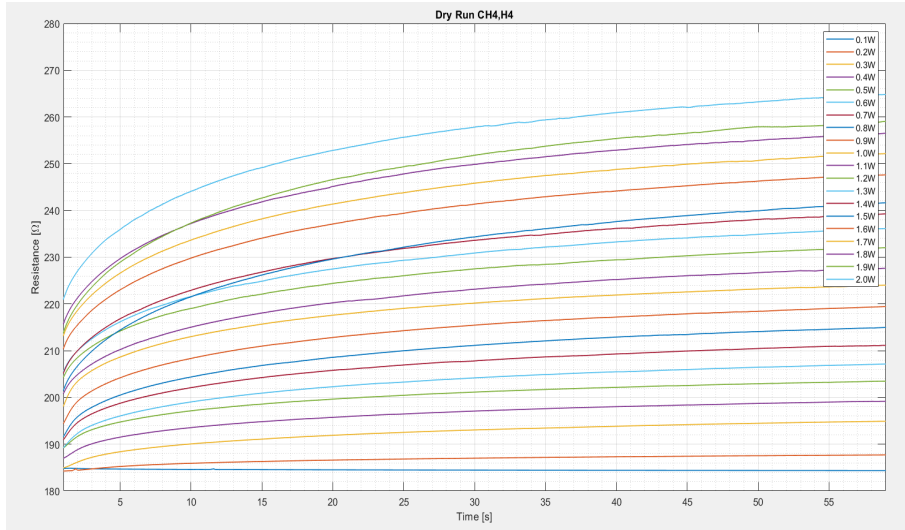


Figure 5.5: Temperature Response of the CH<sub>4</sub> (dry) for the given power input

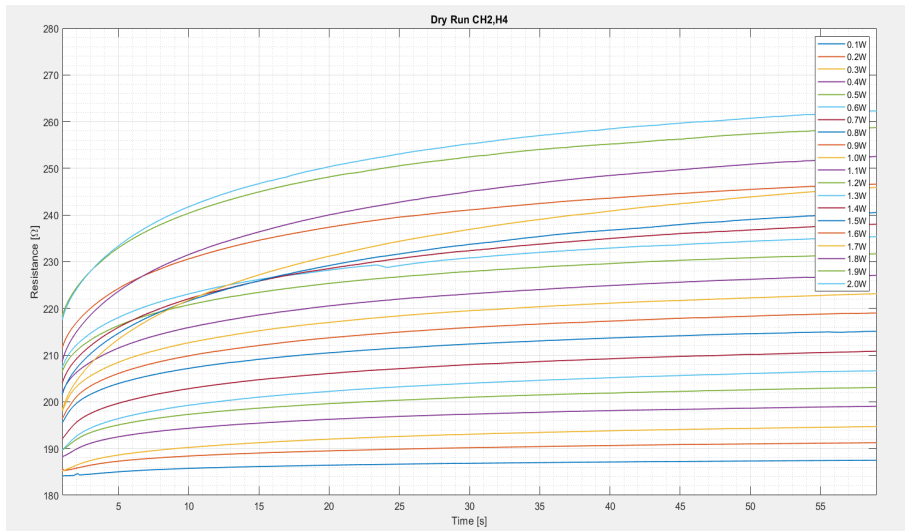


Figure 5.6: Temperature Response of the CH<sub>2</sub> (dry) for the given power input

### Wet run

The same experiment was done with the flow of liquid  $0.25\text{mg/s}$ . The power step, in this case, was a bit bigger due to the difficulty to refill the syringe and reinstalling the chip.

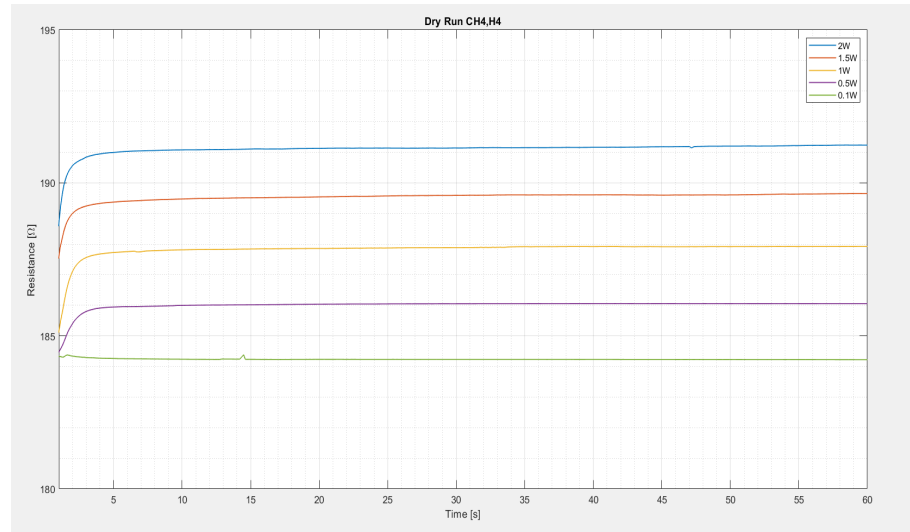


Figure 5.7: Temperature Response of the CH<sub>4</sub> (wet [0.25 g/s]) for the given power input

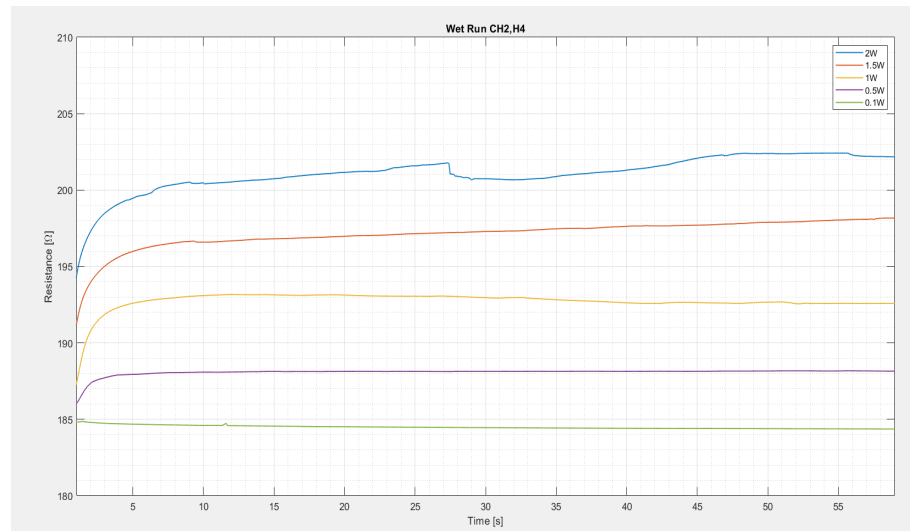


Figure 5.8: Temperature Response of the CH<sub>2</sub> (wet [0.25 g/s]) for the given power input

Heat flux removed by water in a single phase grew linearly by the wall temperature and at  $70^{\circ}\text{C}$  as much as  $400\text{W}/\text{cm}^2$  is expected.

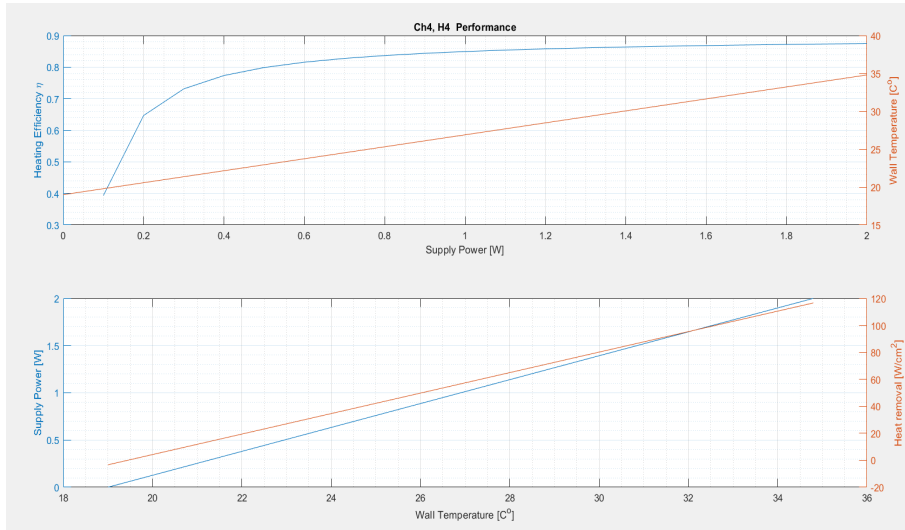


Figure 5.9: Heating efficiency as well as removed heat flux to the propellant at the flow of 0.25g/s

Fin structure	Distance between fins	Heat Flux removed (34C°)
CH <sub>2</sub> (50μm Fins)	50μm	110W/cm <sup>2</sup>
CH <sub>4</sub> (100μm Fins)	100μm	110W/cm <sup>2</sup>

Table 5.2: Heat removal across the channels at 2W

#### 5.2.4 Time constant

Boiling phenomena is accompanied by heater instabilities due to varying heat transfer coefficient during the phase change and as a cause non-uniform heat distribution. In order to mitigate that process heater temperature could be controlled. However, this requires a sharp response of the heater. To make it feasible all the possible DRIE step was taken to remove excess silicon for a more quick response. The increasing volume will reduce the amount of mass that has to be heated and subsequently should result in a fast response time. In addition to it, ambient also affects the rise time of the temperature. When water is present the response time will be much sharper due to the very high heat exchange between the wall and liquid. Aproximate model of the time constant is usually modeled as in the equation 5.2.

$$\tau_1 = \frac{\rho c_p V s}{h A_s} \quad (5.2)$$

As it is expected during the operation with the fluid time constant was much faster. Which could be seen from the figures 5.7 - 5.8. Sharp response of the heaters are quite trivial if the phenomenons taking place inside the chamber has to be known very precisely. As a further research there might be testings on the affect of pulsated heat on the performance of the thruster. For that purpose it might be very useful to even further reduce the heat capacitance beneath the heater and in lateral direction for operating in higher frequency pulses.

### 5.3 PRESSURE DROP ACROSS VARIOUS CHANNEL STRUCTURES

The pressure is very precious for the VLM performance, as thrust is the function of the pressure. Primary design rules of the VLM were built around non-intrusive design, to avoid the pressure drop across the thruster. Information about the pressure gradient across the fin structure is the primary indication of the design quality. Quantitative values recorded across the heater fin structure should reveal pressure variation across the channel while the boiling process is taking place. In order to do so along with inlet, holes for the pressure sensors were etched in the fabrication flow to have mechanical access to the chamber.

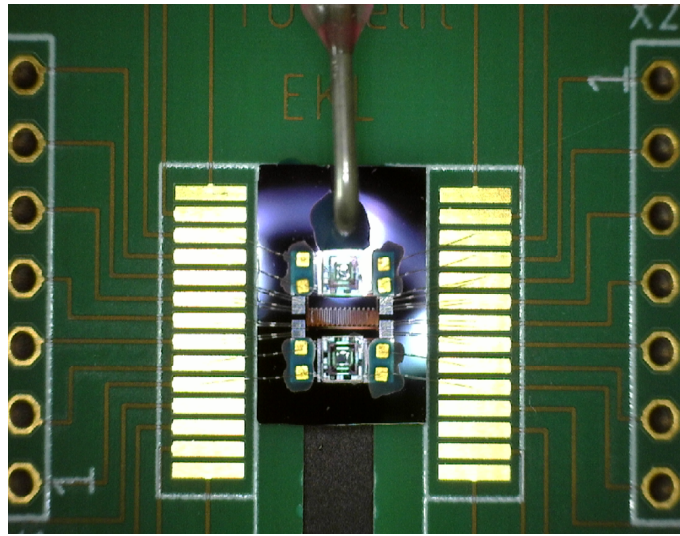


Figure 5.10: EPCOS2013 [10] mounted on top of the VLM

The channel structures used in this design was proven to be poses ability To vaporize the liquid and to further heat the steam up to ( $500C^{\circ}$ ) . For the complete thrusters, the channels need to be characterized by pressure performance. The specific type of thrusters with pressure holes was fabricated and waiting to be tested. Information about pressure fluctuations and overall pressure drop across the channels are a very essential piece of information and for the future work concrete knowledge about pressure performance of the, each channel needs to be precisely known. This would clear the mess around VLM design architecture, as large pressure gradient seriously deteriorates the produced thrust and wastes too much energy. In addition to it to mitigate the boiling instabilities pressure variation and oscillations are extremely important parameters for channel characterization.

## 5.4 VISUAL OBSERVATION

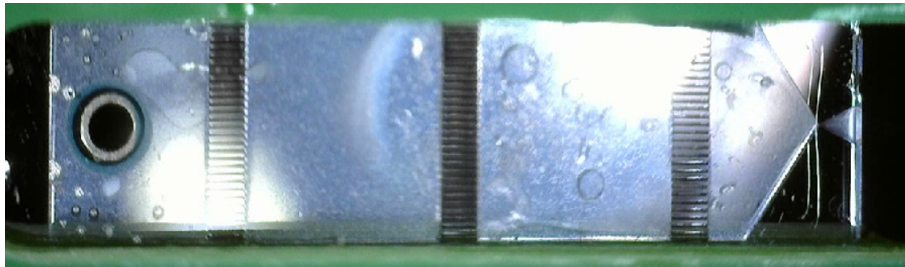
The glass bottom which was made to ensure the transparency for visual observation was made in order to inspect the physical phenomena taking place inside the VLM. The idea of the step-wise heating was to test feasibility to observe the phase change phenomenon in a differentiated by space manner. In other words, each heater is a gate through which the phase change should happen or temperature measurement could be taken. The thermal isolation of the heaters was good enough to make this happen as the thermal capacitance of the etched from the top region were very less to transfer significant heat to the water. In addition to it, the pattern of honeycomb etching made the thermal resistance in the lateral direction much larger.

### 5.4.1 Observation of flow regimes

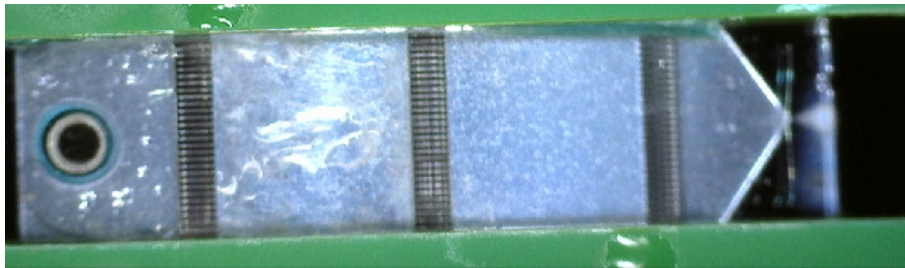
Through the glass wafer videos for various pressure and heat, ranges were collected. Although not analyzed observation of the various flow regimes depending on the pressure versus heat flux was observed and recorded. It was interesting to observe how heat and pressure variation introduced affects the flow regimes.

#### *Liquid flow*

Liquid flow without heating was experimented in the channel. Through this observation, it was noticed that there were no signs of turbulence and uneven flow distribution. All the channels were open (also confirmed by SEM captures of DRIE etching) and a stream of water exiting the nozzle was visually observed for stability.



(a) When only middle heater is working, explosive phase change starting at the middle could be observed at higher flow rates. [0.25 g/s]



(b) When only middle heater is working at it is possible to achieve full phase change at lower flow rates.

Figure 5.11: Visual inspection of flow at high power of 5[W]

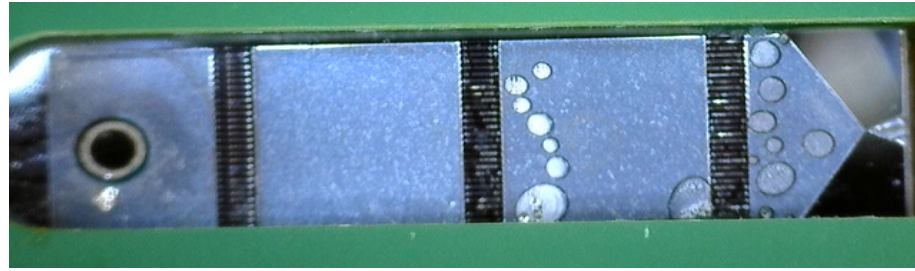


### Gas flow

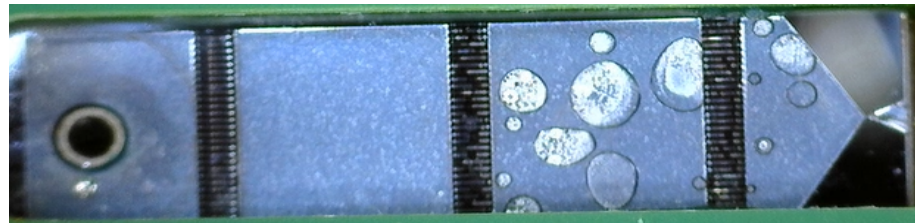
The heating chamber was able to convert the water into gas form as well. In a gas form, the chamber water completely converted into steam and consequent expansion pushed the water out of the chamber. It has to be noted that non-uniform heating is one of the most critical issues of the VLM. There were experiments with highly gassed mineral water with high concentration air molecules which simulated nonuniform heat introduced to the system. In this way, the uneven bubble generation from hot spots could be visualized. Bubbles introduced great instability to the performance of the VLM which could be even observed visually. The stream of the water went in all direction, such an unstable thrust is unacceptable for the safety of the satellite.

### Bubble flow

Liquid and gas flow mixed together was also observed in the heating chamber of the VLM. It was observed that bubble formation is a strong function of the heating. As it differed greatly from the introduced heat operation conditions needs to be predetermined in specified temperature pressure points.



(a) When only middle heater is working bubble is formed only in downstream



(b) Bubbles join each other and gets bigger

Figure 5.12: Visual inspection of bubble formation for the flow rate of  $0.25[\text{g/s}]$  and power supply of  $2[\text{W}]$

#### 5.4.2 Possible Criterion for the flow stability

During the experiments, it was observed that there might be a possibility to achieve flow stability by operating in heat flux condition under which the flow is more stable. This could be backed by the findings of the [32],[36]. One more stability criteria which could be stated is different behavior of the flow when heaters are already at high temperature when the water arrives. It was noticed that when high mass flow which cannot be vaporized arrived at the inlet of the fins it was still vaporized and water didn't move any further despite the pressure increase (even up to  $7[\text{bars}]$ ). Water was

instantly vaporized and subsequent expansion in the chamber didn't allow the further flow of liquid.

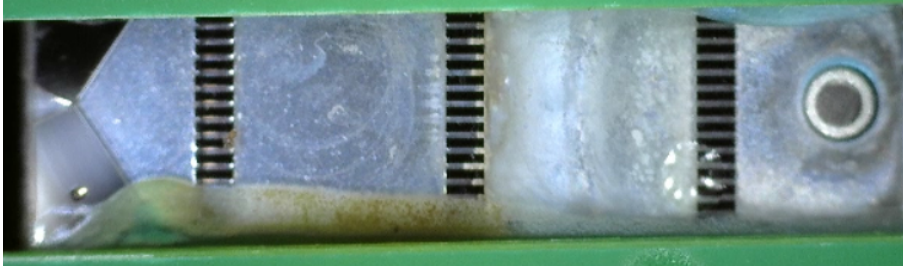


Figure 5.13: Preheated middle heater at  $343^{\circ}\text{C}$  is a gate through which the water is converted into vapour form.

#### 5.4.3 Discussion on wall temperature uniformity

There is a common conception in the VLM design that due to the high conductivity of the silicon, wall temperature across the whole VLM is assumed uniform. However, it has to be noted that it depends on set conditions and heat transfer parameters of the internal microchannel. In this design efforts were spent to achieve constant wall temperature for comfortable calculations and to avoid temperature oscillations, however the wall temperature is constant only for the heater region and the rest of the wall is considered as at the temperature of the liquid due to the isolated structure of the fins and direct placement of the heaters on top of the wall. Most of the silicon above the channels were etched with honeycomb shape to reduce the heat capacity of the wall and to isolate the heaters from all sides to deliver it only to the water. As an example measurement of the heater/RTD readings is presented along with visuals in the figure 5.14.

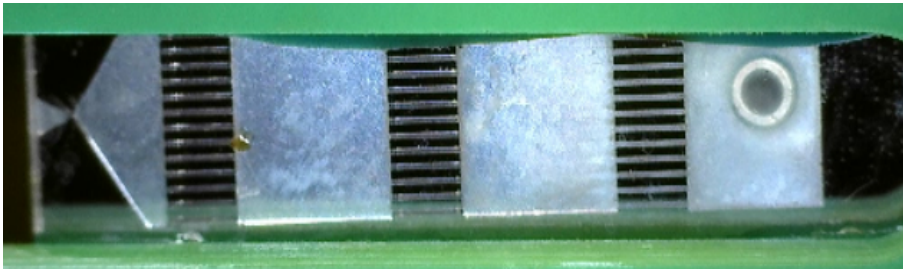


Figure 5.14: When  $6.5[\text{W}]$  was applied to preheat 1st heater (right most) to achieve  $454^{\circ}\text{C}$  the last fin structures (left most wall) showed  $215^{\circ}\text{C}$ .

The proof is overwhelming that there is good thermal insulation along the wall due to the honeycomb structure on top of the channel. Increasing the conduction resistance in lateral direction works and could be implemented on future designs. RTD readings when the 1st heater was working showed more than  $200^{\circ}\text{C}$  temperature difference between the inlet wall and exit wall. The last could be assumed as the temperature of the liquid before exiting the chamber as no power was applied and due to high heat exchange wall will be at the same temperature as vapor.

## 5.5 CHAPTER SUMMARY

The results of RTD calibration and subsequent measurement of the device were presented in this section. It was observed that at a flow rate of  $250\text{mg/s}$  up to  $1\text{MW}/\text{m}^2$  or  $100\text{W}/\text{cm}^2$  at  $34\text{C}^\circ$  were removed from the designed microchannels. In single phase heat flux, up to  $400\text{W}/\text{cm}^2$  at  $70\text{C}^\circ$  could be removed with the same flow rate. Importance of the multi-phase could be observed when operating at  $343\text{C}^\circ$   $300\text{W}/\text{cm}^2$  was removed by water with a flow rate of less than  $2\text{mg/s}$ . It is not hard to see why such a massive heat removal potential of the multiphase system is heavily researched nowadays. With minor improvements in the design very high temperatures up to the melting point of silicon could be achieved with the molybdenum heaters. It would be amazing to see what happens to the water and what kind of specific impulse limits could be achieved. Although Isp saturates at higher Reynolds numbers and no significant performance increases is expected, from a scientific point of view, it will be a great point of interest to see how water will react to such an extreme temperature.

The heaters placed on top of the fin structures were used to measure the wall temperature. Heat sink designed proven to possess effective heat removal quality to remove local heat through fin structures generated from the heater. It possesses quicker thermal response giving the opportunity to combat the unwanted effects of sputtering by trying to affect the temperature according to physical phenomenon taking place inside the microchannels. The design was made with some excess for durability to withstand high pressure (up to 10 [bars]). However, it was observed that there is no need for high pressure for this type of channels to drive the water. Therefore much more silicon could be removed in the future designs to reduce the time constant to achieve sharper temperature response. In addition to it, sputtering which is the main challenge in the design of the multi-phase microchannels proven to be mitigated for the channel types used in the current design. Therefore, this design can be considered as a potential candidate for the future VLM designs.<sup>1</sup>

---

<sup>1</sup> For the testing purposes normal tap water with various ions were used. As a recommendation for the future experiments, deionized, degassed water should be used to have more precise experimental results. From the figures presented it is possible to see residuals build up in the channels which eventually could affect the performance. However, the characterization experiment was conducted on fresh devices and residual ions should not affect the outcome.



# 6 | SUMMARY

## 6.1 CONCLUSION

*"If the end product requires efforts to make it work, the design is wrong !"*

---

H. van Zeijl

This section presents conclusions and includes recommendations for further research. Objectives of the project specified in the introductory chapter are discussed and summarized.

1. Investigate the VLM as a system and describe the performance attributes in a mathematical model. (based on the literature and past projects done in TU Delft).

*Ideal rocket theory along with necessary heat transfer theory was investigated and introduction chapter offers existing models of thruster input-output parameters.*

2. Investigate methods of system orthogonalization into independent parts for straightforward analysis and modular design efforts.

*VLM was decomposed into modules, and modules were further separated into sub-modules for analysis based on literature. In other words, input-output parameters were extracted from the ideal rocket model for all modules and the heating chamber was differentiated to optimize power, thrust performance.*

3. Investigate possible means of improving heating efficiency. (the foremost important task of the research).

*To achieve the foremost desired goal of the project numerous attempts were taken and heat transfer modes were studied to understand how energy is distributed in the VLM. It was concluded that beside improvements of forced convective heat transfer to the propellant, all other heat transfer parameters could be optimized and the process was dedicated towards opening doors to verify that.*

4. Investigate deriving proper heat sink shape or other means of making VLM heating chamber isothermal and stable.

*During the lifespan of the project it was understood that one of the consequences of the design error of the fin structure leads to heater thermal instability. Although attempts could be done to solve this with the introduction of*

*feedback control, correct geometry is still a better solution. Longer the channel, the bigger is the temperature difference in the inlet and outlet end of fins. Therefore, it should be just big enough to deliver the required heat and at the same time preserve thermal stability. Geometry build for this project attempts to achieve this goal by isolating the heater as much as possible from the rest of the silicon bulk blocking it by increasing conductive thermal resistance to the sides and decreasing towards propellant. Among the instability modes, two-phase boiling instability was discussed. This is, however, too complex goal to achieve. Nevertheless, several methods of achieving it were discussed: the introduction of pressure drop elements and non-uniform channel structures for the elevation of the inlet pressure.*

5. Investigate options of achieving a non-intrusive design of chamber for reduction of pressure (thrust) losses.

*Pressure drop in the channel is dictated by the hydraulic diameter of the structure. Therefore, it was concluded to keep it large by fabricating straight ducts and considering options of increasing heat transfer through it.*

6. Investigate solutions of achieving more compact (miniaturized) VLM and subsequent reduction of mass and volume without a reduction in functionality.

*As a result of the power enhancement investigation, it was concluded that forced convective heat is highly dependent on geometry. Therefore an improvement in geometry will allow much more compact design. Pressure goes hand on hand with the length and hydraulic diameter of the chamber. The design of the channels was done in such a manner to downsize the VLM and the resulting structure was more compact as well as with larger hydraulic diameter to keep pressure losses low.*

7. Investigate feasibility of fabrication to achieve the above tasks.

*In this thesis, several fabrication methods were experimented. Novelty, introduced in the thesis is the use of multi-step heater: where several channel structures with different heat transfer characteristics have been fabricated in series, therefore, allowing to propellant receive heat along with the chamber in a step-wise way. Thus, was a measure to reduce rapid heat exchange at the beginning of the channel due to the largest temperature difference between chamber wall and liquid. Among techniques which were experimented were an attempt to remove as much silicon bulk as possible, from the bottom side and from the top. Reducing mass even though not very significant is a step towards fuel economy. However, the main reason for aggressive silicon bulk removal was to reduce the rise time of the temperature and power consumption of the heaters. Demonstrated two side bulk etching is not limit, depending on operating pressure requirements appropriate mechanical structure with optimum thickness and shape could be fabricated in future researches.*

8. Investigate mathematical solutions to describe the behavior of the designed device.

*Simplified finite element numerical model with several input-output assumptions was made and the digital model of the chamber was simulated to predict power transfer mechanisms and based on this model design choices were made.*

9. Investigate back end options(packaging) of the final product without affecting performance in a negative way.

*In most instances packaging reduce functionality in some or other way. However, for VLM it is almost the opposite. Packaging will allow to seal thermal runaway and give durability to the structure. The only drawback is an insignificant increase in mass and cost.*

10. Investigate options for conducting non-intrusive experiment techniques to verify functionality.

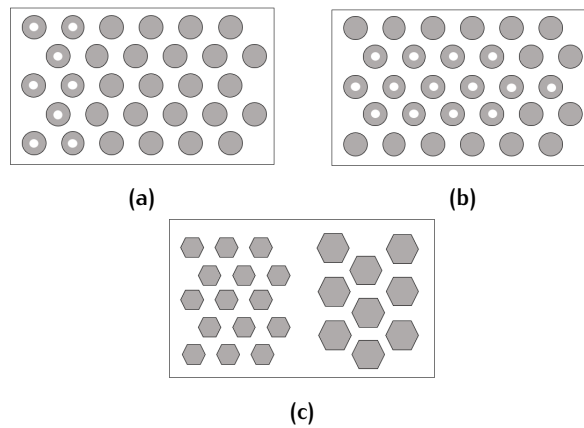
*In order to verify the functionality of the device, the experimental setup was organized. Organized setup was able to input power in the range of 0-5W. Setup also could measure temperature variations along with the chip. In addition to it, the microfluidic interface was connected to the chip to provide a constant supply of the water. Phase change phenomena, as well as the liquid flow in the channel, was experimentally observed and recorded.*

## 6.2 FURTHER RESEARCH

### *Expansion on channel geometry*

Forced convective heat transfer inside the heating chamber directly depends on wall geometry however geometry with same surface contact area doesn't guarantee a rise in heat removal efficiency. This fact was touched in the current work and expansion on this direction could be done to find effective heat sink to suit VLM application even better and even further mitigate some existing problems like explosive boiling and large pressure oscillations. Based on the results of the work it could be suggested that several other geometries could be experimented to find the best shape of the internal wall structure. This, however, should be done with an experienced engineer with a deep understanding of flow and heat transfer simulations. During the project span, numerous heater geometries were considered and abandoned either for fabrication challenges or just inability to fit all of them into mask and test during the limited time given for the project. Furthermore, some geometries considered - required fundamental studies on fluid dynamics and coupling it with electromagnetism and heat transfer physics. Several examples of such structures are illustrated in figure 6.1

Figure 6.1a - Channel geometry with internally hollow structure going all the way to fin base decrease volumetric heat delivered to the fin as thermal resistance of the fin goes up due to a small area of contact. Therefore, this quality could be used to affect Nusselt's number along with the heating chamber. It is known that due to non-perfect thermal insulation thermal path to the liquid is not the same for all fins. Experimentally it was observed in many studies that central fin structures receive more heat due to parasitic heat loss in channel sides (by radiation, convection). In order to combat thus irregular heat delivery method in (a) could be tested as shown in figure 6.1b. It is not necessary to create more fragile hollow structures but instead channels with different geometries could be constructed (figure 6.1c). This would be another mean of controlling Nusselt's number. However, this structure would result in non-uniform pressure drop as hydraulic geometry of the channel is varied along its path to the throat. Despite of intuitive non-attractiveness of the introduction of the non-uniform pressure drop element. It might be useful to test these structures if they can prevent backflow and explosive bubbling.



**Figure 6.1:** (a) - (b) Channel geometry with internally hollow structure (c) Channel geometry with varying structures

### *Integration of all VLM modules*

Although, during this project, functional VLM was fabricated, for DELFFI mission complete reliable product that satisfies all the requirements needs to be accomplished. It is obvious that it is not a task for one Ms thesis. At the moment quite advanced VLM modules were researched in various faculties of TU Delft. Integration of all the existing modules is a task that is waiting to be accomplished. In other words, this could be the next step in a path towards realizing the propulsion system for DELFFI mission.

### *Packaging*

The final product fabricated needs to be packaged for safe handling and for more energy efficiency. There are a variety of options to achieve that. The product has to be worked from two sides from the front end and back end to be suitable for use, as difficult to handle and/or fragile product has little value. Therefore this part of the project has to be researched more in depth as well.

Plenty of packaging options are available for reducing power consumption by thermally insulating the device to reduce energy runaway. One of the options could be GSG (glass silicon glass) sandwich figure 6.2. Two glass wafers could be anodically bonded to the silicon wafer as shown by [29]. The resulting structure could be packaged further by standard procedures like applying mold. This will further solidify thruster performance by creating a very high thermal barrier for energy generated by the resistor.

In addition to it, packaging will introduce a reliable mean of measuring temperature as the top glass wafer will allow fabricating structures which are isolated from conductive heat generated from the heater figure 6.3. Box in green (small) is a temperature sensor while it is almost completely isolated from the heater as conductive properties of the glass are very less, this will allow parasitic effect free liquid temperature measurement. While temperature sensors placed on top of glass wafer (large green) will allow measuring heat loss to the environment.

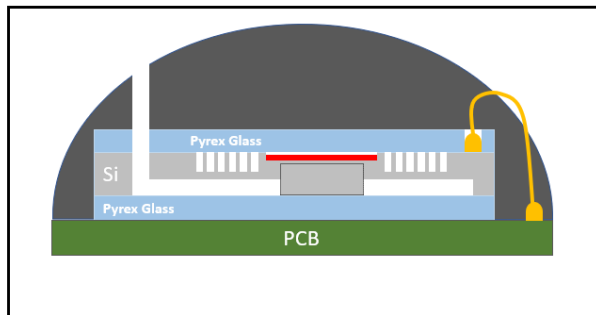


Figure 6.2: Packaged device concept

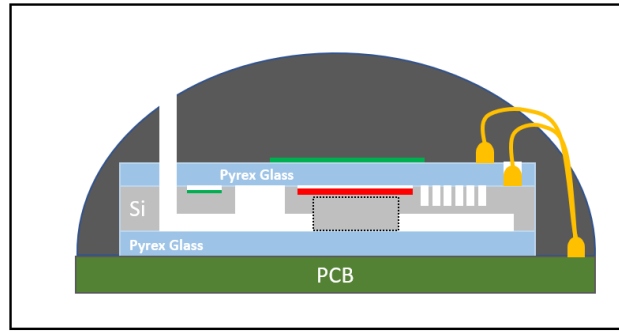


Figure 6.3: Packaged device with temperature sensor

#### *Introduction of control interface (for operation in pulsated mode)*

A very advanced transducers class are called smart sensors is sensors were analog data collected is filtered and analyzed through smart algorithms and based on that feedback loop is introduced to make decisions accordingly. For, instance up to this moment operation in pulsated mode has not experimented. Operations in this mode have the potential to increase heat transfer dramatically due to resonant modes. As now multiple prototype samples of VLM exists it could be an appropriate moment to give them some intelligence and explore possibilities of the pulsated operation mode. Thus requires advanced circuitry and smart programming skills. However, the task is not impossible and could be done as a Ms project. Such research will help to move VLMs into a new level of transducers.

#### *Experimental setup*

One important aspect which was encountered during the project is verification of the heater performance. To control and measure microfluidic phenomenons taking place inside the VLM advanced closed loop setup is required. As a recommendation for the one who will continue the project, it should be noted that specific chamber with controlled inlet and outlet of water and air with controlled pressure environment for both water and air needs to be designed. In addition to it, this small chamber has to have a set of sensors for thrust measurement (strain gauges, or other types of sensitive pressure sensor able to measure thrust in mN range). It will allow rapid and complete characterization of the MEMS heater and MEMS thruster as a whole.

### 6.3 POSSIBLE APPLICATIONS OTHER THAN VLM

**Heat sink (cooling)** - the purpose of the heating chamber is to deliver heat to the propellant or in other words heat needs to be removed by a fluid. Thus the principle of heat removal could be applicable in temperature management of thermal energy generating devices like high power LEDs. Example of such a work could be [37] where liquid cooling of high power LEDs was tested. Application of multiple structure channels could be used to cool down an array of LEDs with different heat generation rate. Cooling by microfluidics is a quite promising choice as an enormous amount of heat ( $10^7 \text{ W/m}^2$ ) by the relatively small mass of water could be removed from the miniature silicon surface by this method. As a widely used current method of removing heat by natural convection to air is approaching its limit and cannot be a suitable solution to ever increasing power density. In addition to it in some instances like space application thus conventional methods are not even possible due to the absence of air [6]. Due to thus reasons in the near future, efficient heat removal will be in high demand, where multi-phase loops will take the superior position due to the ability of water absorbing a large amount of heat to overcome latent heat of evaporation.

**Microfluidics** - Numerous applications in the design of micro-biochips, micro-reactors, and micro-fuel cells require knowledge of heat transfer behavior and pressure variation inside the microchannels. Thermal efficiency improvements in the thermal micro-structures are a point of interest for many scientists and recently high research activity could be noticed from the literature and industries around the world.





## BIBLIOGRAPHY

- COMSOL Multiphysics Manual <http://www.comsol.com>.
- "IEEE IEEE Code of Ethics", Ieee.org Available: <http://www.ieee.org/about/corporate/governance/p7-8.html>.
- Robert Louis Bayt. *Analysis, fabrication and testing of a MEMS-based micro-propulsion system*. PhD thesis, Massachusetts Institute of Technology, 1999.
- H Shea C. Ataman, S. Dandavino. Wafer-level integrated electrospray emitters for a pumpless microthruster system operating in high efficiency ion-mode. *MEMS*, 2012.
- A. Cervone. Propulsion system requirements for the delffi satellites. *TU Delft*, 2013.
- J.F.M. Velthuis C.M. Rops, F. van der Graaf. Micro evaporators. *MEMS, NANO and Smart Systems*, ICMENS Proc. Int.Conf.:on 421–426, 2004.
- S.K.Lahiri D.K.Maurya, S. Das. An analytical model of a silicon mems vaporizing liquid microthruster and some experimental studies. *Sensors and Actuators A: Physical*, 2005.
- M. A. Thomas D.L Hitt, C. M. Zakrzwski. MemS-based satellite micro-propulsion via catalyzed hydrogen peroxide decomposition. *Smart Materials and Structures*, 2001.
- J. Lepkowski E. Haile. Oscillator circuits for rtd temperature sensors. Technical report, Microchip Technology Inc., 2004.
- EPCOS. Absolute pressure sensor for wet media. Technical report, Mouser Electronics, 2013.
- W.-L Chen H.-J. Shaw. Laminar forced convection in a channel with arrays of thermal sources. *Warmeund StoffObertragung*, (26):195–201, 1991.
- C. Hanselaar. Evaporative two-phases micro-flow modelling. Master's thesis, TU Delft, 2016.
- D Teyssieux D Briand N. F. de Rooij J. Courbat, M Canonica. Design and fabrication of micro-hotplates made on a polyimide foil: electrothermal simulation and characterization to achieve power consumption in the low mw range. *Journal of Micromechanics and Microengineering*, 2010.
- M. Meyyappan Jin-Woo Han. A built-in temperature sensor in an integrated microheater. *IEEE SENSORS JOURNAL*, 16(14):5543–5547, 2016.
- Ho-Young Kwak Jung-Yeul Jung. Fluid flow and heat transfer in micro-channels with rectangular cross section. *Heat and Mass Transfer*, 44(9):1041–1049, 2007.
- R. Thorslun J. Kohler M. Boman L. Stenmark K. L. Williams, A. B. Eriksson. The electrothermal feasibility of carbon microcoil heaters for cold/hot gas microthrusters. *JOURNAL OF MICROMECHANICS AND MICRO-ENGINEERING*, 2006.

- S. Ang K. Zhang, S. K. Chou. Mems-based solid propellant microthruster design, simulation, fabrication, and testing. *JOURNAL OF MICROELECTROMECHANICAL SYSTEMS*, 13(2):165–175, April 2004.
- Merck KGaA. Az-12xt-20pl series chemically amplified positive tone photoresists. Technical report, Merck, 2016.
- L. Wang M. Zhou Z. Cui L. Chai, G. Xia. Heat transfer enhancement in microchannel heat sinks with periodic expansion–contraction cross-sections. *International Journal of Heat and Mass Transfer*, 2013.
- M. K. Singha K. M. Subramaniam N. Jampana S. Asokan L. Lakshmi, R. Rao. Molybdenum microheaters for mems-based gas sensor applications: Fabrication, electro-thermo-mechanical and response characterization. *IEEE SENSORS JOURNAL*, (17):22–29, 2017.
- E. Iervolino M. Mihailovica T. Rossia A.T. Trana H. Schellevis J.F. Creemera P.M. Sarro L. Melea, F. Santagata. A molybdenum mems microhotplate for high-temperature operation. *Sensors and Actuators A: Physical*, 188:173–180, 2012.
- H. van Zeijl A.Cervonea E. Gill M.A.C. Silvaa, D. C. Guerrieria. Vaporizing liquid microthrusters with integrated heaters and temperature measurement. *Sensors and Actuators A: Physical*, 2017.
- T. Mathew. Design of a mems-resistojet. Master’s thesis, TU Delft, 2011.
- M. Mihailovic. *MEMS Monocrystalline-Silicon Based Thermal Devices for Chemical and Microfluidic Applications*. PhD thesis, TU Delft, 2011.
- Juergen Mueller. Thruster options for microspacecraft: A review and evaluation of existing hardware and emerging technologies. *Jet Propulsion Laboratory California Institute of Technology*, 1997.
- T. Ziemann D. Telitschkin Hans-Jorg Fecht A. Friedberger N. Miyakawa, W. Legner. Mems-based microthruster with integrated platinum thin film resistance temperature detector (rtd), heater meander and thermal insulation for operation up to 1,000c. *Microsyst Technol*, (18):1077–1087, 2012.
- London A. P. A systems study of propulsion technologies for orbit and attitude control of microspacecraft. Master’s thesis, Massachusetts Institute of Technology, 1996.
- R.M.A. Poyck. Design, manufacturing and characterisation of a water fed cubesat micro-resistojet. Master’s thesis, TU Delft, 2014.
- X. Wang Q. Li. A novel sandwich differential capacitive accelerometer with symmetrical double-sided serpentine beam-mass structure. *Journal of Micromechanics and Microengineering*, 2016.
- A.L. London R.K. Shah. Laminar flow forced convection in ducts, adv. heat transfer, supplement 1. Technical report, New York, 1978.
- M. Abassi P. Enoksson S. Rahiminejad, P. Cegielski. A four level silicon microstructure fabrication by drie. *Journal of Micromechanics and Microengineering*, 2016.
- C.G. Piero S.K. Saha. *Instability in flow boiling in microchannels*. Springer, 2016.

- D.B. Tuckerman. High-performance heat sinking for vlsi. *EEE Electron Device Letters*, 2(5):126–129, 1981.
- T. X. VanWees. Characterization and testing of a memsvaporizing liquid microthruster for small satellite propulsion. Master's thesis, TU Delft, 2017.
- Z. Li S. Li Q. Liu C. Xu H. Wan X. Wu I. P. Dong I. Design, fabrication and characterization of a solid propellant micro-thruster. *Conference on Nano/Micro Engineered and Molecular Systems*, pages 476–479, January 2009.
- P. Bhandari Y. K. Prajapati. Flow boiling instabilities in microchannels and their promising solutions – a review. *Experimental Thermal and Fluid Science*, 2017.
- H. Ye. *Thermal management of Solid State Lighting Module*. PhD thesis, TU Delft, 2014.





## APPENDIX A (DELFFI REQUIREMENTS)

Propulsion System Requirements for Delffi Mission as shown in [5]:

- **PROP-PERF-100:** The total Delta-V provided by the propulsion system shall be at least 15 [m/s].
- **PROP-PERF-200:** The thrust provided by the propulsion system shall be above 0.5 [mN].
- **PROP-PERF-205:** The thrust provided by the propulsion system shall be below 9.5 [mN].
- **PROP-PERF-400:** The propulsion system shall have a lifetime of at least 1 year under operational conditions in space.
- **PROP-PERF-410:** The propulsion system shall be able to withstand at least 5000 on-off cycles without losing its capability to meet any other performance or system requirement.
- **PROP-SYST-100:** The total wet mass of the propulsion system at launch shall be not higher than 459 [g].
- **PROP-SYST-200:** The total size of the propulsion system shall be within 90 [mm] x 90 [mm] x 80 [mm]
- **PROP-SYST-310:** The peak power consumption of the propulsion system during ignition or heating shall not be higher than 10 [W].
- **PROP-SYST-320:** The total energy consumption of the propulsion system shall be no more than 100 [kJ] per day (i.e. 1.1574 [W] daily average).
- **PROP-SYST-410:** The nominal geometrical axis of the nozzle shall be perpendicular to the plane of one of the smaller faces (100 [mm] x 100 [mm]) of the satellite.
- **PROP-SYST-500 to PROP-SYST-560:** The propulsion system shall be able to withstand the launch loads.
- **PROP-SYST-600:** The internal pressure of all propulsion system components shall not be higher than 10 [bar].
- **PROP-SYST-610:** The propulsion system shall not include any pyrotechnic devices.
- **PROP-SYST-620:** The propellant(s) used by the propulsion system shall not be hazardous for the operators or the other satellite sub-systems.
- **PROP-SYST-710:** The thermal interface between the propulsion system and the satellite shall maintain a temperature range between -20 [C] and 80 [C] for the propulsion system components during all the mission phases when propulsion system operations are required.
- **PROP-SYST-720:** The propulsion system shall be electrically connected to the satellite power sub-system through the standard cubesat I2C interface.



# B | APPENDIX B (FLOW CHART)

In this Appendix fabrication flow is attached

1. CLEANING:  $\text{HNO}_3$  99% and 69.5% (OPTIONAL)
2. COATING
3. EXPOSURE
4. DEVELOPING
5. INSPECTION: Linewidth and overlay
6. PLASMA ETCHING: Alignment markers (URK's) in Silicon
7. LAYER STRIPPING: Photoresist
8. CLEANING:  $\text{HNO}_3$  99% and 69.5%
9. DRY OXIDATION
10. MEASUREMENT: OXIDE THICKNESS
11. LPCVD  $\text{SiN}_3$  (500nm)
12. MEASUREMENT: NITRIDE THICKNESS
13. Mo SPUTTERING
14. LAYER SHEET RESISTANCE MEASUREMENT
15. PECVD TEOS DEPOSITION (300nm)
16. MEASUREMENT: TEOS THICKNESS
17. COATING
18. EXPOSURE
19. DEVELOPING
20. INSPECTION: Linewidth and overlay
21. Dry Etching PECVD TEOS
22. INSPECTION
23. MEASUREMENT: TEOS THICKNESS
24. DRY ETCHING (MOLYBDENUM)
25. LAYER STRIPPING: Photoresist
26. TRITON (Surface Preparation)

27. BHF wet etching
28. INSPECTION
29. MEASUREMENT: TEOS THICKNESS
30. PECVD TEOS (600nm)
31. MEASUREMENT: TEOS THICKNESS
32. COATING
33. EXPOSURE
34. DEVELOPING
35. INSPECTION: Linewidth and overlay
36. Dry Etching PECVD TEOS (window opening)
37. INSPECTION
38. MEASUREMENT: TEOS THICKNESS
39. TRITON (Surface Preparation)
40. BHF wet etching
41. MEASUREMENT: TEOS THICKNESS
42. LAYER STRIPPING: Photoresist
43. IDC 1um Al layer sputtering SIGMA – IDC layer
44. CLEANING PROCEDURE: HNO<sub>3</sub> 100% (metal)
45. COATING– SPR<sub>3012</sub> – IDC layer
46. EXPOSURE
47. DEVELOPING
48. INSPECTION: Linewidth and overlay
49. Dry Etching Al
50. LAYER STRIPPING: Photoresist
51. CLEANING PROCEDURE: HNO<sub>3</sub> 100% (metal)
52. LAYER STRIPPING: Nitride and Thermal Oxide (BACKSIDE)
53. MEASUREMENT: OXIDE THICKNESS
54. PECVD TEOS DEPOSITION (HARD MASK)
55. MEASUREMENT: TEOS THICKNESS
56. COATING (Backside for hard mask patterning)
57. EXPOSURE
58. DEVELOPING
59. INSPECTION: Linewidth and overlay



60. Dry Etching PECVD TEOS
61. MEASUREMENT: TEOS THICKNESS
62. Dry Etching LPCVD Nitride (on inlet and pressure sensor holes)
63. MEASUREMENT: Nitride THICKNESS
64. LAYER STRIPPING: Photoresist
65. CLEANING PROCEDURE: HNO<sub>3</sub> 100% (metal)
66. COATING
67. EXPOSURE
68. DEVELOPING
69. INSPECTION: Linewidth and overlay
70. Dry Etching PECVD TEOS
71. MEASUREMENT: TEOS THICKNESS
72. CLEANING PROCEDURE: HNO<sub>3</sub> 100% (metal)
73. COATING (backside soft mask)
74. EXPOSURE
75. DEVELOPING
76. INSPECTION: Linewidth and overlay
77. DRIE
78. INSPECTION: 3D microscope analyser
79. LAYER STRIPPING: Photoresist
80. CLEANING PROCEDURE: HNO<sub>3</sub> 100% (metal)
81. DRIE
82. INSPECTION: 3D microscope analyzer
83. CLEANING PROCEDURE: HNO<sub>3</sub> 100% (metal)
84. PECVD TEOS DEPOSITION (Landing Layer)
85. MEASUREMENT: TEOS THICKNESS
86. CLEANING PROCEDURE: HNO<sub>3</sub> 100% (metal)
87. COATING (front side soft mask)
88. EXPOSURE
89. DEVELOPING
90. INSPECTION: Linewidth and overlay
91. DRIE
92. INSPECTION: KEYENCE 3D microscope analyzer

93. TRITON (Surface Preparation)
94. BHF wet etching (Backside Hard Mask removal)
95. MEASUREMENT: TEOS THICKNESS
96. INSPECTION: No residuals of TEOS
97. LAYER STRIPPING: Photoresist (from front side)
98. CLEANING PROCEDURE:  $\text{HNO}_3$  100
99. ANODIC BONDING
100. DICING
101. GLUING DEVICE INTO PCB
102. WIRE BONDING
103. ELECTRICAL CHARACTERIZATION

## C | APPENDIX C (HEATERS & CHANNELS )

Several heaters designed for thruster application is presented here. Numbering used in this section is consistent throughout the work and done to avoid confusion. Dimensions of the heaters and channels could be found from table C.1

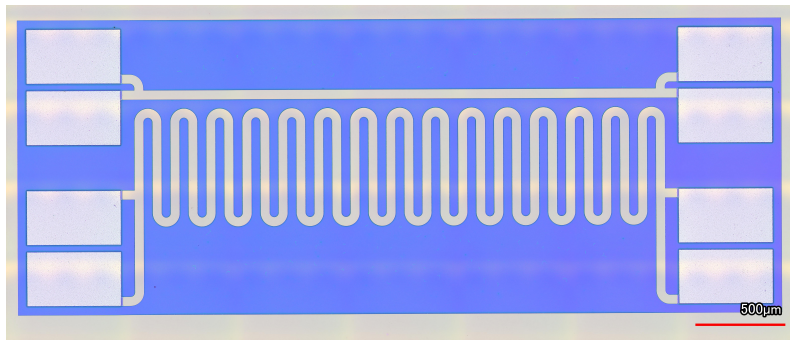


Figure C.1: Heater 1

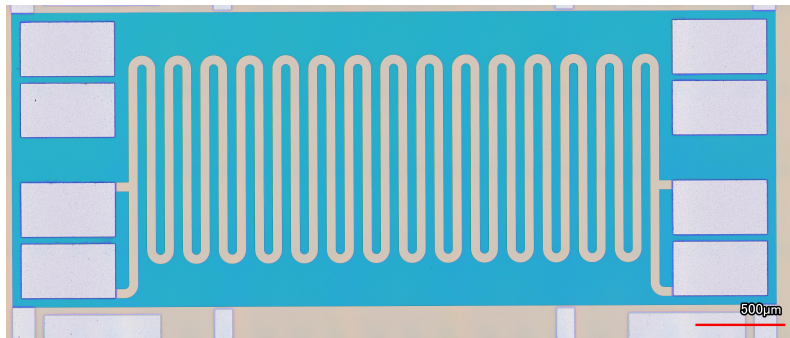


Figure C.2: Heater 2

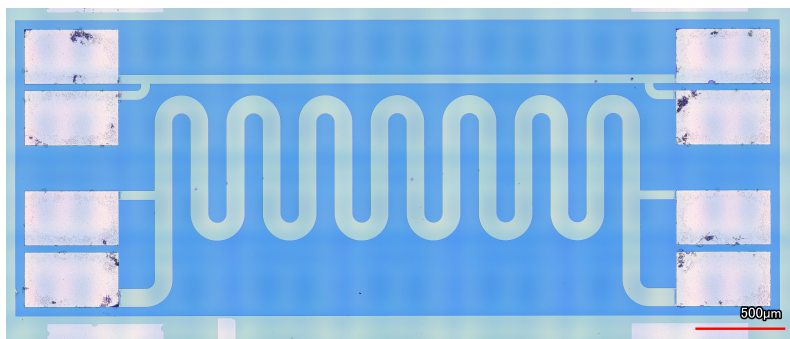


Figure C.3: Heater 3

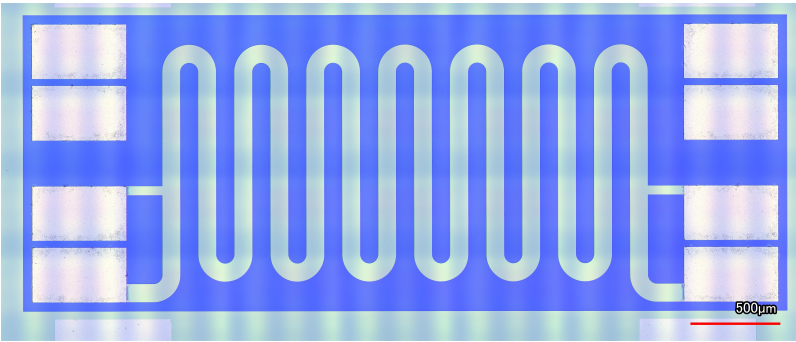


Figure C.4: Heater 4

#	Heater 1 (H1)	Heater 2 (H2)	Heater 3 (H3)	Heater 4 (H4)
W	50µm	50µm	100µm	100µm
H	500µm	1000µm	500µm	1000µm
R [ohm] (20C <sup>0</sup> )	370Ω	660Ω	100Ω	160Ω

Table C.1: Table with nomenclature and description of a heaters here H is length of one meander

The same procedure will be used for the channels and (fin-structures). Nomenclature and description of the dimensions could be found form the table ??.

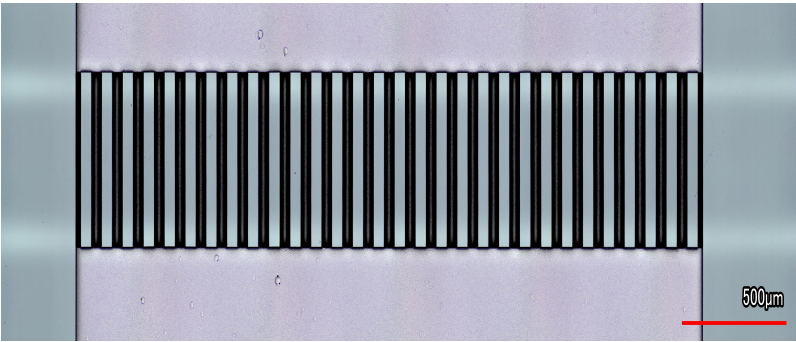


Figure C.5: Channel 1 Microscope capture

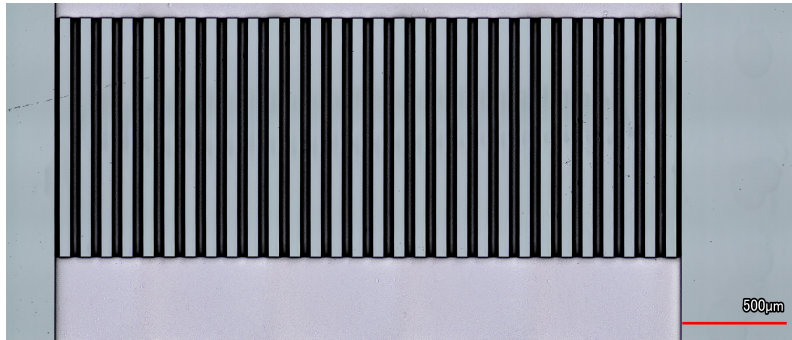


Figure C.6: Channel 2 Microscope capture

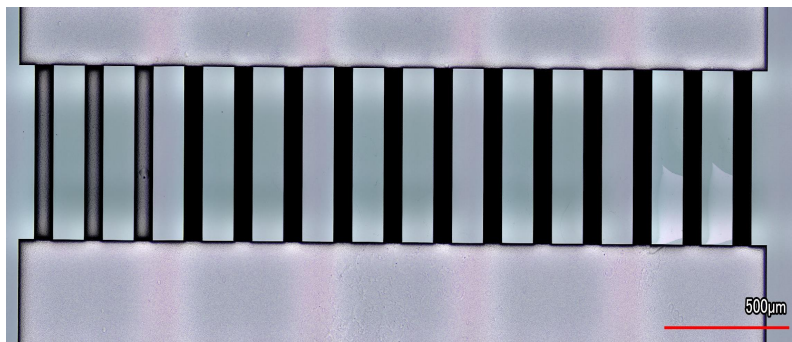


Figure C.7: Channel 3 Microscope capture

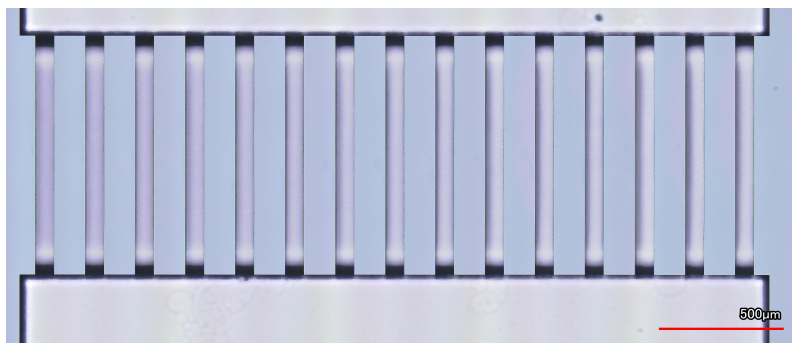


Figure C.8: Channel 4 Microscope capture

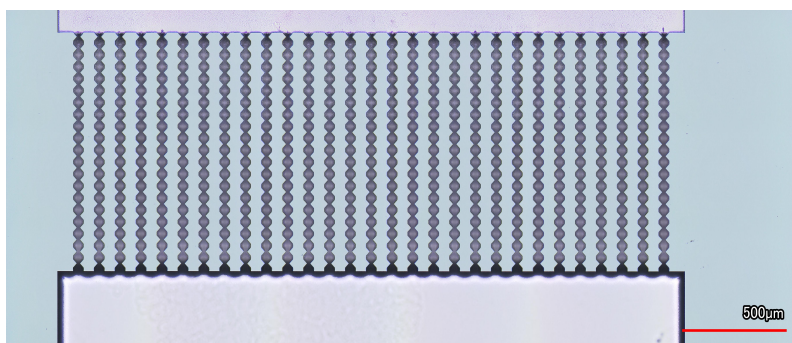


Figure C.9: Channel 5 Microscope capture



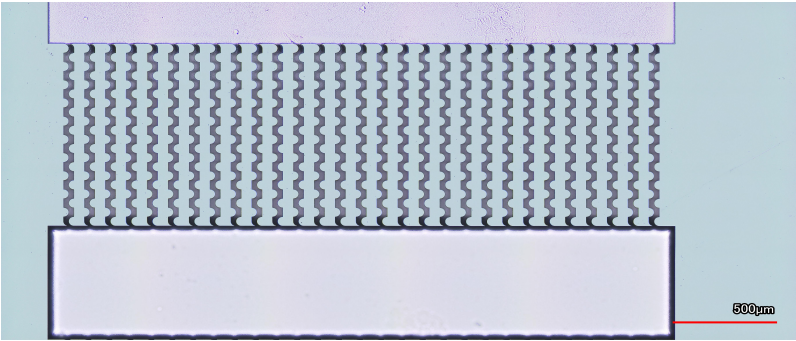


Figure C.10: Channel 6 Microscope capture

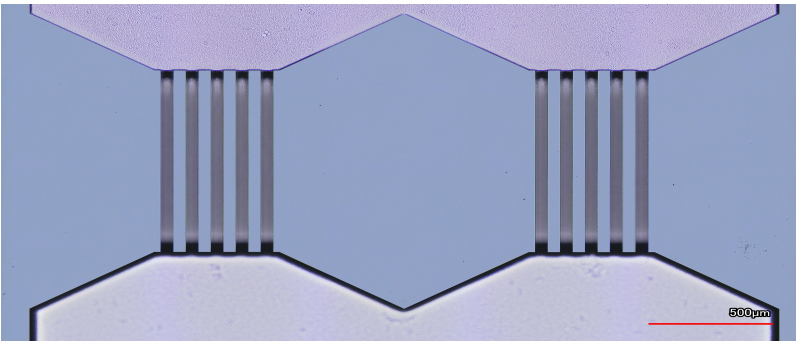


Figure C.11: Channel 7 Microscope capture

Channel #	Width	Length
Channel 1 (C1)	50μm	500μm
Channel 2 (C2)	50μm	1000μm
Channel 3 (C3)	100μm	500μm
Channel 4 (C4)	100μm	1000μm
Channel 5 (C5)	varies	1000μm
Channel 6 (C6)	varies	1000μm
Channel 7 (C7)	varies	1000μm

Table C.2: Table with nomenclature and description of a channels

# D | APPENDIX D (MASK )

In this appendix mask designed for fabrication of the device is presented. For lithography exposure each cell with size of 1625 [ $\mu\text{m}$ ] by 4250 [ $\mu\text{m}$ ] rectangle was a building block for specific module. Mask is made to be able to assemble any combination of channel & heater giving flexibility in fabrication. Combinations, extracted for this thesis are listed below the mask.

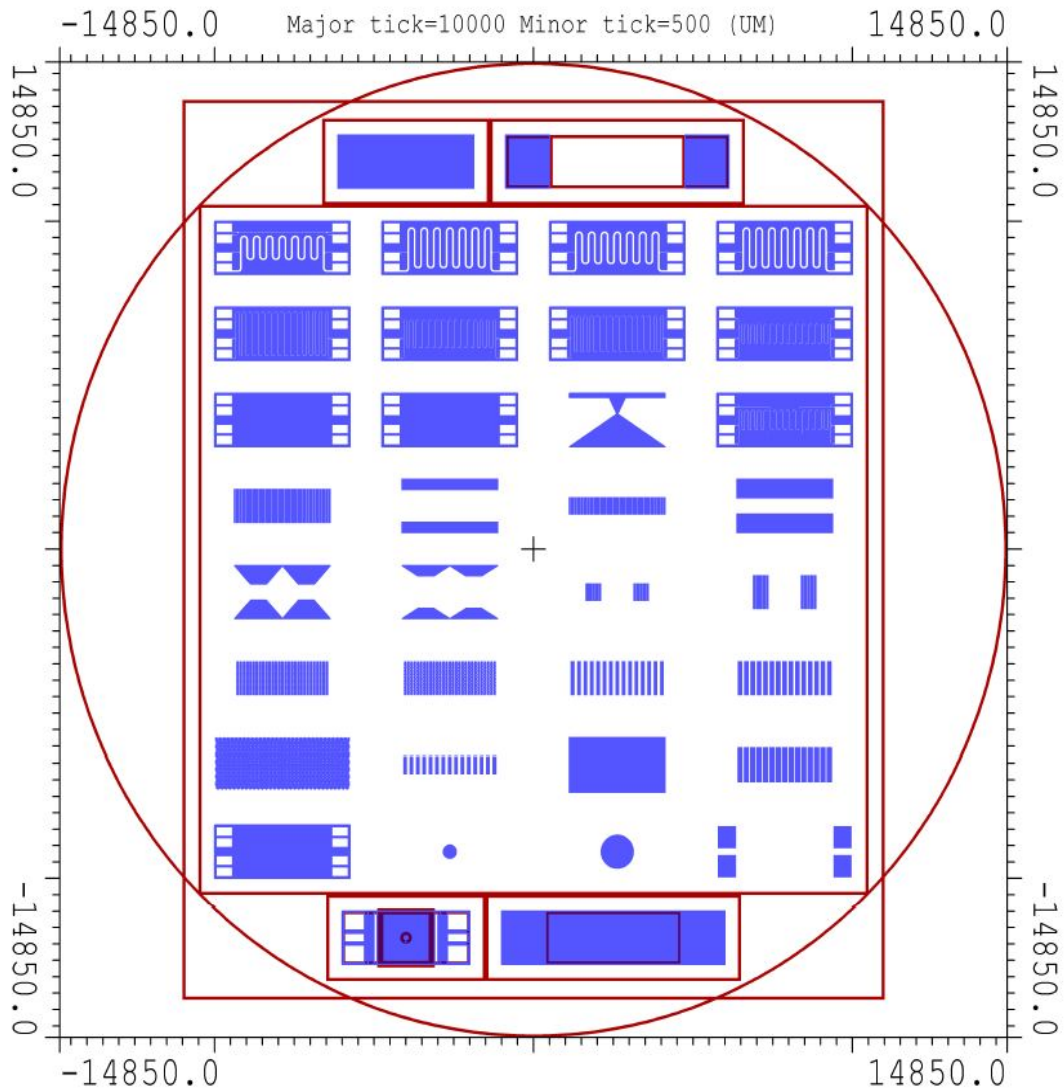
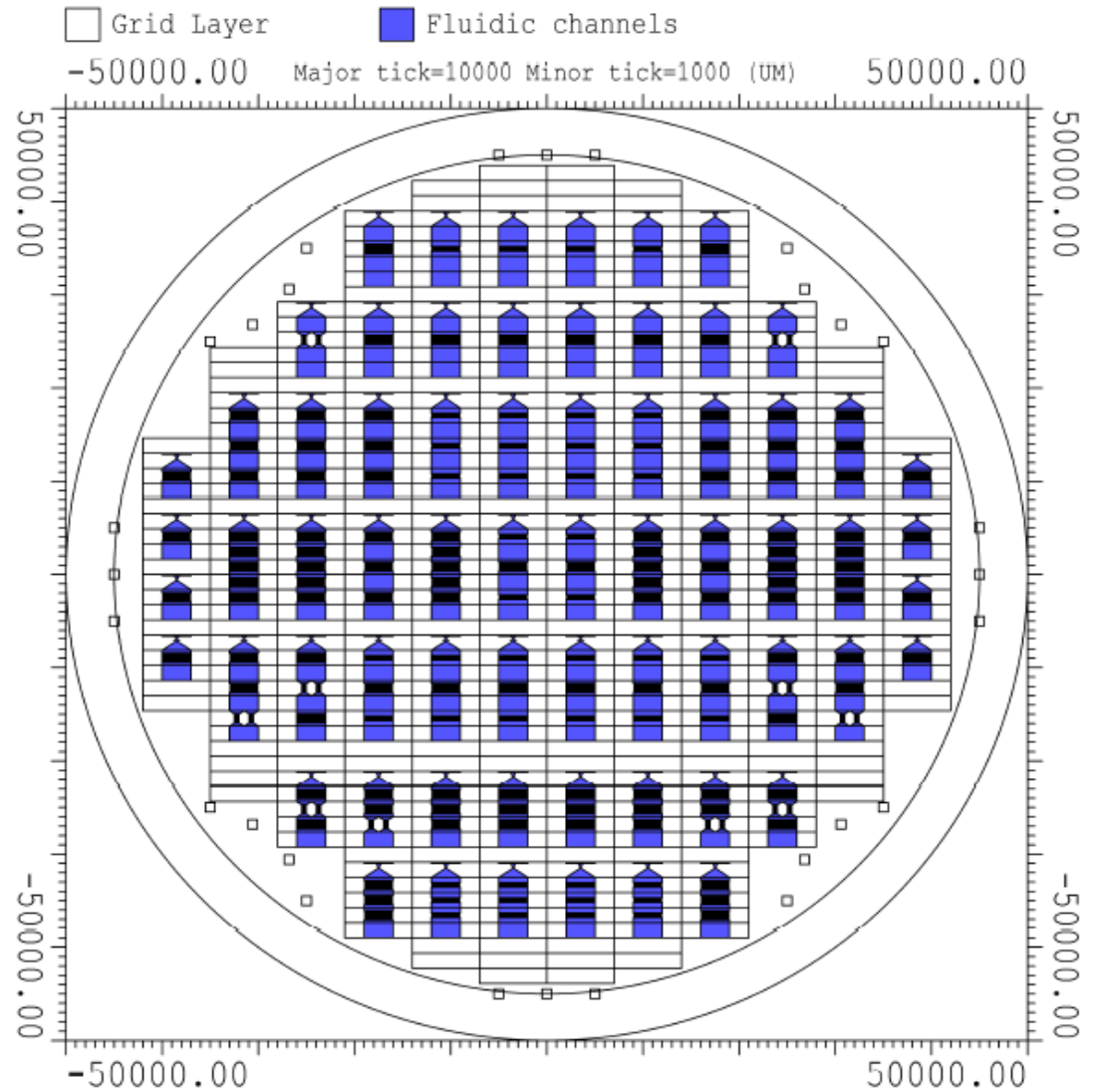


Figure D.1: Mask Top Cell



**Figure D.2:** Wafer level organization of the devices. Each square inch of the wafer was attempted to be used to get max amount of devices. Wafer is organized in a symmetric way around y axis to avoid lithography errors in alignment. Proposed combinations are not limit and if desired much bigger thrusters could be assembled.



Note: not all combinations have been tested due to limited resources available as all the chips needs to be installed to package in our case to PCB.

1. Combination type 1 - Each channel is fabricated separately. This was done to test individual structure for heat transfer efficiency as well as for pressure drop.
2. Combination type 2 - Here same type of channels are carved in the silicon three times with a expanding hollow channel section for free flow of the liquid.
3. Combination type 3 - Here same channels are etched five times with smaller gap in between.
4. Combination type 4 - Several type of channels alternated with gap in between.
5. Combination type 5 - Two types of channel structures are placed and there is a blockade of very narrow section to supply necessary pressure drop in case of pressure drop is too small and liquid is pushed from chamber without receiving necessary energy.



# E | ETHICS

Ethics is an important aspect of our project and we have strived to maintain the highest level of ethics, as has been mandated in the IEEE Code of Ethics [2]. We will follow all of it but these points will be our main concern.

(1) to accept responsibility in making decisions consistent with the safety, health, and welfare of the public, and to disclose promptly factors that might endanger the public or the environment;

Our project involves interaction with water and this may cause unwanted exposure of our electrical parts to water. To ensure that our end user is safe, appropriate sealing of the mechanical and electrical parts were accomplished. In addition to its materials which tend to degrade while under direct contact with water were isolated from it.

(3) to be honest and realistic in stating claims or estimates based on available data; to improve the understanding of technology; its appropriate application, and potential consequences;

We have been honest with our calculations, methodologies, research, and conclusions. The work is fully repeatable based on the report presented and any data confirming it can be accessed from this report. Furthermore, if questions arise we will be happy to provide any additional information.

(6) to maintain and improve our technical competence and to undertake technological tasks for others only if qualified by training or experience, or after full disclosure of pertinent limitations;

In this project, the fabrication of MEMS device was accomplished under strict requirements and numerical calculations were made to forecast the behavior of the system. Thus, would be tested by qualified university personal and validity of the work will determine whether it can be defended to obtain Ms. Degree.

(7) to seek, accept, and offer honest criticism of technical work, to acknowledge and correct errors, and to credit properly the contributions of others;

We have made mistakes while creating this project and have done all that we possibly can to learn from our mistakes and create a product that reflects this.





"The head of a man is a **mind**, a leader is an **incentive**, an analyst is a **thought**, a companion is a **profession**, a fortress is a **patience**, a guardian - **character**."

(Kazakh Proverb)

Science enhances the moral value of life, because it furthers a love of truth and reverence — love of truth displaying itself in the constant endeavor to arrive at a more exact knowledge of the world of mind and matter around us, and reverence, because every advance in knowledge brings us face to face with the mystery of our own being.

(Max Planck)

The only purpose of the education is Freedom; the only method Experience.

(Leo Tolstoy)

We are asleep until we fall in love.

(Leo Tolstoy)

Your actions are representation of who you are, you cannot run from yourself.

(from cartoon "Samurai Jack")



